

146
301
THS

AN ANALYSIS OF OVERLAND FLOW

Thesis for the Degree of Ph. D.

MICHIGAN STATE UNIVERSITY

Chen-lung Chen

1962

THESIS

RY
Michigan State
University

MICHIGAN STATE UNIVERSITY
LIBRARY

~~XXXXXXXXXX~~ LIBRARY JUN 3 7 1963

Circulate June 30

MICHIGAN STATE UNIVERSITY
LIBRARY

~~XXXXXXXXXX~~
~~XXXXXXXXXX~~

MSU

AN ANALYSIS OF OVERLAND FLOW

By

Chen-lung Chen

AN ABSTRACT OF A THESIS

Submitted to
Michigan State University
in partial fulfillment of the requirements
for the degree of

DOCTOR OF PHILOSOPHY

Department of Agricultural Engineering

1962

Approved Ernest H. Kiddle

ABSTRACT

AN ANALYSIS OF OVERLAND FLOW

by Cheng-lung Chen

The differential equations of continuity and of motion of a somewhat simplified version of the overland flow problem have been arranged to permit computation of particular solutions by means of a digital computer. Approximate evaluations of some of the terms in the equation of motion were necessary, however, the results of the computations would indicate that except for the resistance to flow these terms have only a minor influence on the phenomenon.

The simplified overland flow problem investigated consisted of the flow on an impervious sloping plane with a vertical wall at the upstream end and a free overfall at the lower end due to a constant rain. The approach could easily be modified to accommodate variable rain and surface characteristics and different controls.

The particular conditions for which computations have been carried out demonstrate how the various factors can be studied to find their effect on the flow. The results of the computations which have been made tend to confirm the unit hydrograph concept, and even suggest that a universal dimensionless hydrograph might be a practical

approximation. More computations are needed to explore this possibility and to provide the auxiliary time relationship needed to make it a workable tool.

AN ANALYSIS OF OVERLAND FLOW

By

Cheng-lung Chen

A THESIS

Submitted to
Michigan State University
in partial fulfillment of the requirements
for the degree of

DOCTOR OF PHILOSOPHY

Department of Agricultural Engineering

1962

Approved Ernest A Kidder

VITA

Cheng-lung Chen
candidate for the degree of
Doctor of Philosophy

Final examination: August 3, 1962; 3:00 P. M. ; Room 119
Agricultural Engineering Building

Dissertation: An Analysis of Overland Flow

Outline of studies:

Major subject: Agricultural Engineering
Minor subjects: Civil Engineering
Mathematics

Biographical items:

Born: November 1, 1931; Taichung, Taiwan, China

Undergraduate studies: National Taiwan University, B. S. , 1954
Michigan State University, M. S. , 1960
Michigan State University, 1960-1962

Experience: Junior Engineer, Irrigation Section, Design Division,
Water Conservancy Bureau, Provincial Taiwan Govern-
ment, 1955-1958

Graduate Research Assistant, Agricultural Engineering
Department, Michigan State University, 1958-1962

Special Graduate Research Assistant, Division of
Engineering Research, Michigan State University, 1962

Professional affiliations: Member of

Chinese Society of Agricultural Engineers
Chinese Society of Hydraulic Engineers
American Society of Agricultural Engineers

ACKNOWLEDGEMENTS

The author wishes to express his sincere thanks to Professor Ernest H. Kidder of Agricultural Engineering Department, under whose constant supervision and unflinching interest this investigation was undertaken.

The author expresses his sincere gratitude to Dr. Emmett M. Laursen of the Civil Engineering Department, whose inspiration, stimulating advice, and dynamic guidance made this study possible.

Sincere thanks are extended to Dr. A. W. Farrall and the Division of Engineering Research providing the opportunity and financial assistance for the pursuance of this program of studies.

Grateful acknowledgements are extended to Dr. Charles P. Wells of Mathematics Department and Dr. Merle L. Esmay of the Agricultural Engineering Department for their serving on the guidance committee.

A special note of thanks is due Dr. Harold R. Henry of the Civil Engineering Department for his valuable assistance and suggestions.

TABLE OF CONTENTS

Section	Page
STATEMENT OF THE PROBLEM	1
FORMULATION OF THE PROBLEM	8
The flow equations	8
The boundary values and controls	13
PROCEDURE OF SOLUTION	22
Finite-difference scheme	22
Digital computer routines	26
RESULTS AND DISCUSSION	32
CONCLUSIONS	42
REFERENCES	44
APPENDIX	67
Nomenclature	67

LIST OF FIGURES

Figure		Page
1.	General sketch of overland flow problem	4
2.	The diagram of the fluid element abcd under external forces and momentum fluxes	4
3.	Segment of flow under rainfall intensity r	10
4.	Sketch of a mixed flow	20
5.	Relating curves among S_o , n , q_c^* , r , and L_c	21
6.	The solution surfaces in the x - t - y and x - t - u spaces cut by 4 planes $x = x_i$, $x = x_{i+1}$, $t = t_j$, and $t = t_{j+1}$	25
7.	Definition sketch for the method of finite-difference	25
8.	Sketch of flow profiles determined by trial-and-error method	30
9.	Profiles of water depth with time as a parameter during rainfall	45
10.	Profiles of water depth with time as a parameter in the receding stage	46
11.	Stage-hydrographs for different positions on the slope ...	47
12.	Profiles of the mean velocity along the surface with time as a parameter during rainfall	48
13.	Profiles of the mean velocity along the surface with time as a parameter after rainfall	49
14.	Velocity-hydrographs with distance as a parameter	50
15.	Discharge-profiles with time as a parameter during rainfall	51
16.	Discharge-profiles with time as a parameter in the receding stage	52

Figure		Page
17.	Discharge-hydrographs for various distances along the surface	53
18.	Relationship between velocity and depth with distance and time as parameters	54
19.	Relationship between discharge and depth with distance and time as parameters	55
20.	Comparison of discharge-hydrographs due to different intensities of rainfall	56
21.	Comparison of discharge-hydrographs due to different roughnesses at the overfall	57
22.	Comparison of depth-hydrographs due to different roughnesses at the upstream end	58
23.	Comparison of discharge-hydrographs due to different slopes	59
24.	Comparison of discharge-hydrographs due to different inclinations of rainfall	60
25.	Comparison of discharge-hydrographs at $x = 30$ ft. due to different lengths of channel	61
26.	Comparison of depth-hydrographs at $x = 30$ ft. due to different lengths of channel	62
27.	Dimensionless discharge at the overfall q/rL against the dimensionless time $t/t_{1/2}$	63
28.	Dimensionless discharge q/rx against the dimensionless time $t/t_{1/2}$	64
29.	Depth-profiles of a mixed flow	65
30.	Stage-hydrographs of a mixed flow.....	66

LIST OF TABLES

Table		Page
1.	Subcritical runs	32

STATEMENT OF THE PROBLEM

The general overland flow problem is the case of flow resulting from a rainfall varying in space and time falling on a pervious surface of large areal extent which varies in slope, roughness, and infiltration rate. The overland flow which results from the net rain, moreover, would be unsteady and non-uniform even if these elementary quantities were not variables. If the rain falls for a very long time period at a constant rate, the flow approaches a limiting state which is steady, but non-uniform, with the rate of flow at every point equal to the integral of the rain falling upstream from the point. Before this limit is reached, storage is occurring so that the depth of flow and the rate of flow are changing with time as well as space.

Overland flow is important in a variety of situations; firstly, it is an important element in surface runoff and, therefore, the flood flow of streams. In particular, highway and airport engineers are interested because the overland flow phenomenon determines the depth of water on the pavement and the required drainage facilities to accept the flow from operational areas. The agricultural engineer is particularly interested in a variation of this problem in irrigation flooding where infiltration is equivalent to a negative rain, as well as in respect to drainage and erosion problems.

The analysis presented herein represents a simpler version of the general problem in that the flow is two-dimensional, the surface is impervious, the rainfall is constant both spatially and temporally, and the slope and resistance to flow (as represented by the Manning's n value) are constant. However, the procedure, or computer program, evolved would need only additional simple sub-routines to accept variable slope, roughness, and rainfall, without any change in the basic program. If the infiltration could be considered as a function of space and time and independent of the depth of flow, this factor could be included simply as modifying the rainfall rate.

A schematic sketch of overland flow is shown in Fig. 1. If critical depth occurs at the downstream end all of the time, the flow everywhere must be subcritical; otherwise, a mixed condition with subcritical flow upstream and supercritical flow downstream of a critical channel control can be expected. The position of the critical section for the mixed flow is a function of the slope, the roughness, and the rate of flow, and therefore, of space and time. The critical depth has been taken as one of the controlling conditions of the flow in this study. Other comparable controls would be possible; for example, a pool could form at the downstream end of a sub-critical slope -- the controlling water surface elevation would then depend on the geometry of the pool and the outflow from the pool. The free overfall was chosen as being simpler in

concept because the critical control is dependent only on the rate of flow and the channel properties. Given any other comparable control the routine of computation could easily be modified.

For the computations, the initial condition has been taken as a dry surface; any arbitrary, but possible, flow could have been used. Although the routine could accept various initial conditions, this consideration would seem to needlessly add complexity at this time.

Another condition that has been used is a velocity of zero at the beginning of the slope. Physically this implies that there is a vertical wall at the beginning of the slope or a symmetrical watershed divide. Again other possibilities exist, such as an arbitrary inflow, but this would seem to be a needless complication that could be added later.

The flow is subject to forces such as gravity, pressure, drop impact, and boundary shear. Considering the fluid element abcd as shown in Fig. 2, the resultant of these forces in the x direction must equal the increase of momentum flux within the element plus the net flux of momentum out of the element in unit time.

$$\frac{\partial M}{\partial t} dt + \frac{\partial M}{\partial x} dx - \rho v \sec \phi \sin (\theta + \phi) = W \sin \theta dx - \frac{\partial P}{\partial x} dx - \tau dx \quad (1)$$

where

M = momentum flux of the element in the x-direction,

W = weight of the element per unit length,

P = pressure force on a normal section of the element,

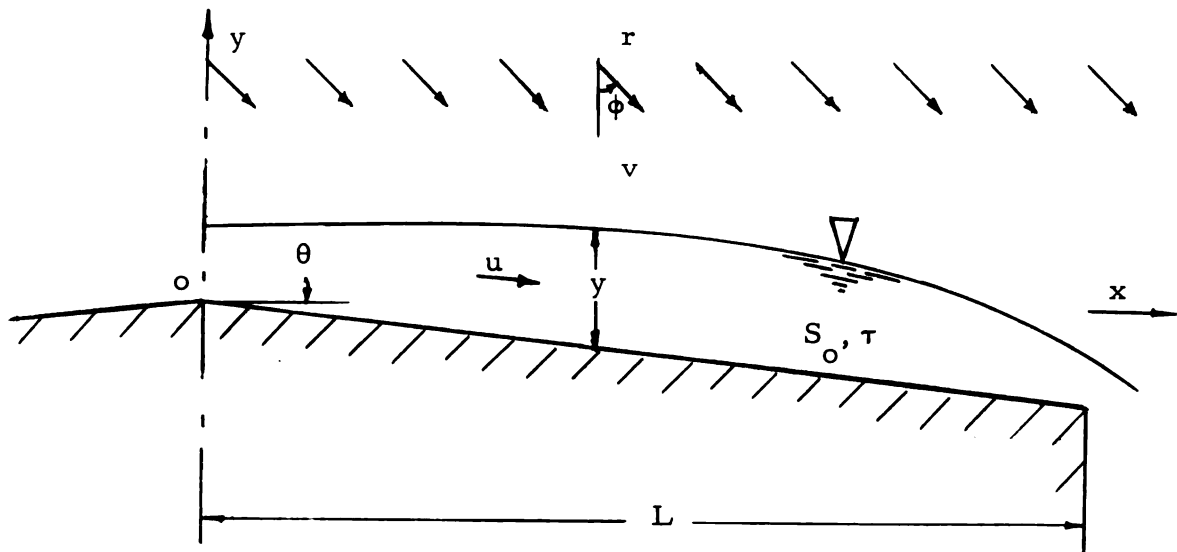


Fig. 1. General sketch of overland flow problem.

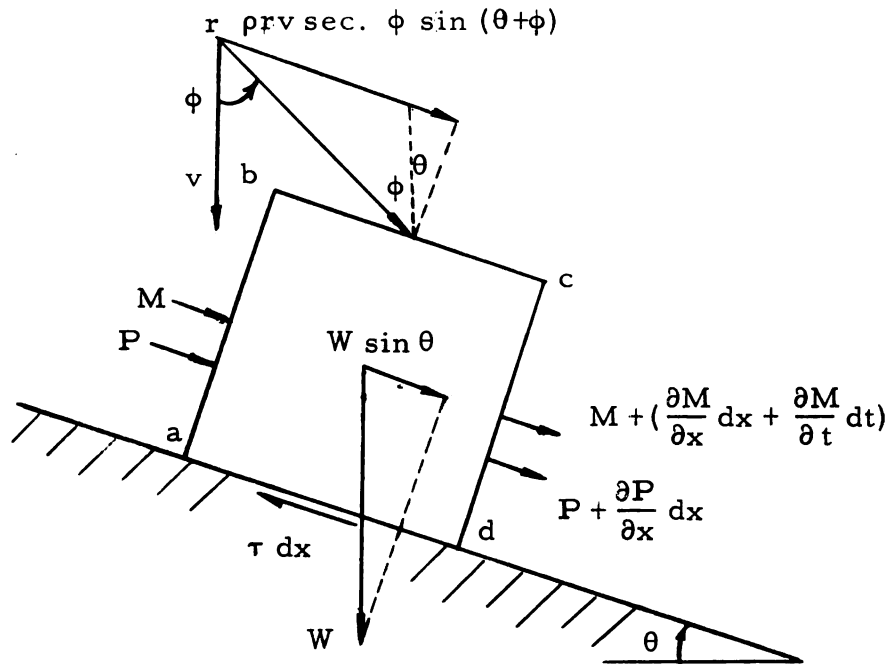


Fig. 2. The diagram of the fluid element abcd under external forces and momentum fluxes.

τ = boundary shear on the element per unit length,

ρ = density of fluid,

r = intensity of rainfall,

v = velocity of raindrops in y direction,

ϕ = angle of rainfall with respect to the vertical, and

θ = angle of inclination of the surface.

The equation of continuity, which must also be satisfied, can be written for this case as

$$\frac{\partial y}{\partial t} + \frac{\partial q}{\partial x} = r \quad (2)$$

where y is the depth of flow and q is the discharge per unit width.

The companion problem of routing floods through river channels has received considerable attention over the years [2, 3]. Less attention has been paid to the overland flow problem, but the work of Izzard [4], Iwagaki [5], and Liggett [6] can be cited as examples of attempts to solve this problem. In some respects the river is a simpler problem than overland flow because the inflow is at one or, at the most, a few points although the geometry can be more complex. The many flood routing procedures can be classified as hydrologic (those utilizing the equation of continuity and a relationship between the storage and the discharge) and hydraulic (those utilizing the equation of continuity and an equation of motion, usually the energy equation). Both procedures

can be questioned on fundamental grounds because of the assumptions that are necessary to obtain solutions [7]; nevertheless, if the assumptions are based on measurements of what happens to the river during flood, they can provide acceptable results.

The weak point of the hydrologic procedures, of course, is the substitution of a storage-discharge relationship for the equation of motion. Such a relationship must be a product of the conditions imposed on the flow, and if a reasonably simple expression is to be a useful approximation, the factors controlling or governing the flow cannot be too variable. Using assumptions based on his experimental measurements, Izzard achieved an analysis which can be classified as hydrologic, and which provides a useful solution within the range of the conditions of his experiments.

The difficulty of solving the hydraulic equations has led various investigators to make various simplifying assumptions. The technique termed the method of characteristics, for example, implicitly assumed that the flood wave travels in respect to the flow at the velocity of a shallow water wave. Iwagaki found the method of characteristics too laborious for general use in the overland flow problem and resorted to two approximate methods that appear to check the more strict solution, at least for very steep slopes. Liggett, basing his analysis on the theory of characteristics, evolved a method of solution which is partly

exact (except for the usual approximations describing the flow) and partly approximate, and which leans heavily on graphical aids.

FORMULATION OF THE PROBLEM

The flow equations. As shown in Fig. 1, when the rain falls with an intensity r , a velocity of the raindrops v , and an angle ϕ (positive if in the same direction as the flow) on the impervious surface of a long and wide plane having a principal slope S_0 and length L , an unsteady, non-uniform flow will occur in the direction of the principal slope with depth y , velocity u , and boundary shear τ variable with the distance x and the time t . To insure two-dimensionality not only must the surface be plane and the x direction taken in the direction of maximum slope, but the rain cannot have a cross component to the direction of flow.

Considering the net flow into element $abcd$ in Fig. 3, and the change in storage, a continuity equation can easily be expressed. The quantity of fluid flowing into the element of unit width in the differential time dt is

$$(q - \frac{1}{2} \frac{\partial q}{\partial x} dx) dt + r dt dx$$

and the amount flowing out is

$$(q + \frac{1}{2} \frac{\partial q}{\partial x} dx) dt$$

The difference between the flow in and out must equal the amount of storage in the time dt

$$\frac{\partial y}{\partial t} dt dx$$

Simplifying and dividing each term by $dt dx$ will give the continuity equation, hence

$$\frac{\partial y}{\partial t} + \frac{\partial q}{\partial x} = r \quad (2)$$

Since $q = uy$, Eq. (2) can be written as

$$\frac{\partial y}{\partial t} + y \frac{\partial u}{\partial x} + u \frac{\partial y}{\partial x} = r \quad (3)$$

As expressed by Eq. (1), the resultant force in the x direction must equal the time rate of increase of momentum within the element $abcd$ plus the net flux of momentum out in unit time.

The resultant force on the element is, for the unit width,

$$W \sin \theta dx - \frac{\partial P}{\partial x} dx - \tau dx$$

The first term is simply the component of the weight of the fluid in the direction of motion

$$W \sin \theta dx = \gamma y \sin \theta dx$$

Making the usual assumption concerning resistance, that the shear is equal to that of a uniform flow of the same depth and velocity on a surface having the required slope of S_f , the last term can be expressed as

$$\tau dx = \gamma y S_f dx$$

In addition to the usual assumption of a hydrostatic pressure force $\frac{1}{2} \gamma y^2$, the pressure term P is assumed to contain the effect of a uniform pressure intensity due to impact from raindrops, so that there is a

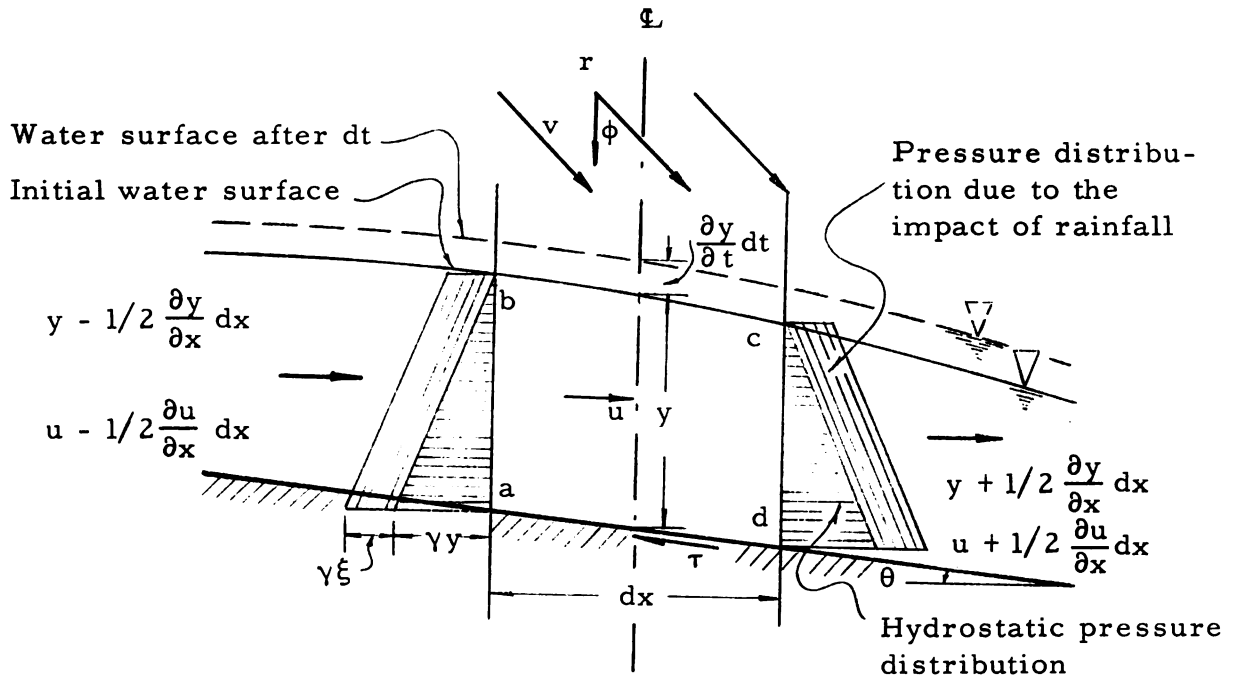


Fig. 3. Segment of flow under rainfall intensity r .

supplementary pressure force $\gamma\xi y$. The value of ξ is assumed to be constant everywhere and throughout the rain, and can be estimated on the assumption that the overpressure is equal to the vertical component of the momentum flux of the rain, hence

$$\xi = \frac{\rho r v}{\rho g} = \frac{r v}{g} \quad (4)$$

Now the pressure force P can be written as

$$P = \rho g \cos \theta \left(\frac{1}{2} y^2 + \xi y \right)$$

both portions of pressure distribution being shown in Fig. 3. In order to evaluate this assumed effect of the rain, or ξ , the fall velocity v of the raindrops must be known.

The resultant force on the element is thus

$$\rho g \sin \theta y dx - \rho g \cos \theta \frac{\partial}{\partial x} (1/2 y^2 + \xi y) dx - \rho g S_f y dx$$

The excess of momentum per unit time leaving cd over that entering ab is

$$\frac{\partial}{\partial x} (\beta \rho u^2 y) dx = \beta \rho u^2 \frac{\partial y}{\partial x} dx + 2 \beta \rho u y \frac{\partial u}{\partial x} dx$$

where β = momentum coefficient, which is dependent on the velocity distribution.

The time rate of increase of momentum within abcd is given by

$$\frac{\partial}{\partial t} (\rho u y) dx = \rho u \frac{\partial y}{\partial t} dx + \rho y \frac{\partial u}{\partial t} dx$$

The rain entering the element will contribute a momentum flux term due to its velocity component in the direction of flow

$$\rho v \sec \phi \sin(\theta + \phi) dx$$

Assembling the force and momentum terms, dividing out dx and ρy , there results

$$\begin{aligned} & \frac{u}{y} \frac{\partial y}{\partial t} + \frac{\partial u}{\partial t} + \beta \frac{u^2}{y} \frac{\partial y}{\partial x} + 2 \beta u \frac{\partial u}{\partial x} - v \frac{r}{y} \sec \phi \sin(\theta + \phi) \\ & = g \sin \theta - g \cos \theta \left(1 + \frac{\xi}{y}\right) \frac{\partial y}{\partial x} - g S_f \end{aligned} \quad (5)$$

Substituting from Eq. (3)

$$\beta \frac{u^2}{y} \frac{\partial y}{\partial x} = \beta \frac{u}{y} \left(r - \frac{\partial y}{\partial t} - y \frac{\partial u}{\partial x}\right) = \beta u \frac{r}{y} - \beta \frac{u}{y} \frac{\partial y}{\partial t} - \beta u \frac{\partial u}{\partial x}$$

for the third term on the left in Eq. (5), finally, there results

$$\begin{aligned} \frac{\partial u}{\partial t} + \beta u \frac{\partial u}{\partial x} - (\beta - 1) \frac{u}{y} \frac{\partial y}{\partial t} + g \cos \theta \left(1 + \frac{\xi}{y}\right) \frac{\partial y}{\partial x} \\ = g (\sin \theta - S_f) + [v \sec \phi \sin(\theta + \phi) - \beta u] \frac{x}{y} \end{aligned} \quad (6)$$

Equation (6) is a general momentum equation which, together with the equation of continuity, Eq. (3), must be solved for y and u as functions of x and t .

To continue, several of the quantities must be evaluated by means of reasonable approximations. For mathematical simplicity, β has been assumed to be unity in most previous studies. Since the flow is assumed to be turbulent, the average value of the usual range from 1.03 to 1.07 for fully developed, steady, uniform open channel flow, namely, 1.05 will be employed in this analysis.

Although the Manning formula was developed empirically for steady, uniform flow, it is a usual and a reasonable approximation for the unsteady, non-uniform flow, if changes are gradual. It is usually felt that any deviation from the steady, uniform shear can be compensated for by a judicious choice of the n value. In this case the choice of the n value should also compensate for any effect of the rain on the boundary shear. The "friction" slope is assumed to be that of a wide channel,

$$S_f = \left(\frac{n}{1.49}\right)^2 \frac{u^2}{y^{4/3}} \quad (7)$$

If θ is very small, $\sin \theta$ approaches S_o , and

$$\cos \theta \rightarrow 1$$

and $\sec \phi \sin (\theta + \phi) \rightarrow \tan \phi$

Meteorologists have found that the size and shape of raindrops, the intensity of rain, and the fall velocity of the drops are interrelated. Measurements by Laws [1], for an intensity of rainfall equal to 2 inches per hour, would indicate an average size of raindrop of 0.1 inch in diameter and a fall velocity of approximately 26 feet per second. This is the value of v which has been used.

Equation (6) can now be written as follows:

$$\begin{aligned} \frac{\partial u}{\partial t} + \beta u \frac{\partial u}{\partial x} - (\beta - 1) \frac{u}{y} \frac{\partial y}{\partial t} + g \left(1 + \frac{\xi}{y}\right) \frac{\partial y}{\partial x} \\ = g(S_o - S_f) + (\tan \phi v - \beta u) \frac{r}{y} \end{aligned} \quad (8)$$

$$\begin{aligned} \text{or } \frac{\partial u}{\partial t} + 1.05 u \frac{\partial u}{\partial x} - 0.05 \frac{u}{y} \frac{\partial y}{\partial t} + \left(32.2 + \frac{rv}{y}\right) \frac{\partial y}{\partial x} \\ = 32.2 (S_o - S_f) + (26 \tan \phi - 1.05 u) \frac{r}{y} \end{aligned} \quad (9)$$

where S_f is expressed as in Eq. (7). The equation used by Liggett could be obtained by assuming $\beta = 1$, $\xi = 0$, and $\tan \phi v = u$.

The boundary values and controls. Although there are many possible variations of the boundary conditions, the scope of the problem had to be limited for this study. Therefore, specific

boundary conditions are treated herein with the purpose of developing general principles and indicating a method of solution. The same problem with other boundary conditions may be attacked by the same methods using obvious extensions of the general theory.

Since Eqs. (3) and (8) are a pair of the first order nonlinear and non-homogeneous partial differential equations in two dependent variables, y and u , to obtain a solution four condition-statements are necessary. These conditions will be concerned with

- (1) $y = y(t)$ or $u = u(t)$ at $x = 0$.
- (2) $y = y(x)$ at $t = 0$.
- (3) $u = u(x)$ at $t = 0$.
- (4) The fourth condition may take several forms, involving one or both dependent variables at $x = x_c$ or $x = L$ in order to uniquely determine a solution.

The initial conditions, the second and the third, could be taken as any possible known flow. The case which has been treated is that of no flow at all, i. e., $y = 0$ and $u = 0$ at $t = 0$.

The first condition has been taken as $u = 0$ at $x = 0$ for all t . This is physically equivalent to saying that there is a vertical wall at $x = 0$ or a symmetrical peak.

The last boundary condition is probably the most crucial. To obtain a well-defined solution it has been assumed to be a critical flow

condition. However, the position of the critical section is dependent on whether the flow is generally sub-critical, super-critical, or mixed. The definition of critical condition is also of concern. The usual definition a Froude number of unity is

$$u = \sqrt{gy} = c \quad (10)$$

where c = celerity of a shallow water gravity wave.

With the effect of rainfall, the conditions at the critical section are more complex than implied by Eq. (10); not only is the velocity not uniform but the pressure is not hydrostatic. A better approximation of the criterion for critical flow would be

$$u = \sqrt{g(y + \xi)/\beta} \quad (11)$$

For simplicity one could approximate Eq. (11) by Eq. (10) because β is close to unity, ξ is relatively small for the larger depths of flow, and the two effects tend to be compensating. Similarly, in curvilinear flow where the pressure distribution is non-hydrostatic, the critical depth as given by Eq. (10) may not be a good approximation of the critical depth as defined by minimum energy. Such an effect is fortunately local and can usually be ignored.

Various boundary conditions could be considered for each of the flow cases as follows:

Subcritical flow. If the bed slope is very small, the flow will be subcritical and the following conditions of interest:

- (a) $u = \sqrt{gy} = c$ at $x = L$, where the slope terminates in a free overfall at $x = L$.
- (b) $y = y_n$ at $x = L$, where the rainfall terminates at $x = L$ but the slope continues and y_n is the normal depth of flow on the slope.
- (c) $y = y(t)$ at $x = L$, where the flow is pooled at $x = L$. The first condition, the free overfall, has been considered herein.

Supercritical flow. It is difficult to imagine a supercritical flow everywhere unless there is a critical or supercritical inflow at $x = 0$. For a very steep slope and no inflow, critical conditions at $x = 0$ ($u = 0, y = 0$) may be an acceptable approximation, but strictly there will be a mixed flow. Iwagaki used this assumption. If the rain terminates at L , but the slope continues, there will be a "backwater" curve approaching the normal depth. If the flow is pooled at $x = L$, and the pool elevation is greater than the sequent depth a jump will occur somewhere on the slope. The control for all of these possibilities, however, would be at $x = 0$.

Mixed flow. The mixed flow of greatest interest is subcritical at the beginning and supercritical at the lower end. At the beginning of the rain, the rate of flow is extremely small and must be subcritical throughout. In time, if the rate of flow becomes large enough (depending on the slope, the length, and the resistance) the condition $u = \sqrt{gy}$ at $x = L$ cannot be satisfied and the critical section moves gradually

upstream from the free overfall. A boundary condition can still be written at the point of critical section, namely

$$u = \sqrt{gy} = c \text{ at } x = x_c$$

In order to locate the critical section on the slope, it is necessary to describe, or assume, some hydraulic characteristics of the flow. At the critical section, it is understood that $S_f = S_c$, $y = y_c$, $u = u_c$, and $q = q_c$. Therefore, from Eq. (7), we have

$$S_c = \left(\frac{n}{1.49}\right)^2 \frac{u_c^2}{y_c^{4/3}}$$

likewise, from Eq. (10),

$$u_c = \sqrt{gy_c}$$

Combining these two equations will give S_c in terms of y_c , u_c , or q_c respectively as follows:

$$S_c = \left(\frac{n}{1.49}\right)^2 \frac{g}{y_c^{1/3}} \quad (12)$$

$$S_c = \left(\frac{n}{1.49}\right)^2 \frac{g^{4/3}}{u_c^{2/3}} \quad (13)$$

$$S_c = \left(\frac{n}{1.49}\right)^2 \frac{g^{10/9}}{q_c^{2/9}} \quad (14)$$

For the given channel slope S_0 and resistance coefficient n , we have the maximum critical depth y_c^* , maximum critical velocity u_c^* ,

and maximum critical discharge q_c^* . Replacing S_c by S_o in Eqs. (12), (13), and (14)

$$y_c^* = \left(\frac{n}{1.49}\right)^6 \frac{g^3}{S_o^3} \quad (15)$$

$$u_c^* = \left(\frac{n}{1.49}\right)^3 \frac{g^2}{S_o^{3/2}} \quad (16)$$

$$q_c^* = \left(\frac{n}{1.49}\right)^9 \frac{g^5}{S_o^{9/2}} \quad (17)$$

Now considering a channel with the given S_o and n under a rainfall intensity r , there will be a subcritical flow with a critical section at the overfall when the rain has just begun. As time goes on, it is of interest to note the change in S_c , which decreases from infinity when $q = 0$, to some finite value as q at the overfall increases, and finally approaches a limiting value as the flow approaches a steady state. If this limiting value of S_c is larger than S_o , the flow is always everywhere subcritical except at the overfall. If as q increases at the overfall, S_c becomes equal to S_o , the critical depth of flow is the normal depth of flow, and q at the overfall equals q_c^* . A greater q at the overfall cannot naturally exist under critical conditions and so the control will shift upstream to where $q = q_c^*$. At this time, the condition $S_o = S_c$ enables us to locate the critical section, that is, to determine $x = x_c$ which

approaches to L_c as a limit as the flow approaches its steady state. At this limiting steady state the maximum discharge, at the overfall, must be rL . Whether we will have a partially supercritical flow can be determined simply by comparing rL with q_c^* . If

$$q_c^* > rL \quad (18)$$

then the flow will be subcritical. If

$$q_c^* < rL \quad (19)$$

supercritical flow will occur for some distance upstream of the overfall. If only rainfall intensity r is known, then we can calculate L_c by setting

$$q_c^* = rL_c \quad (20)$$

Hence

$$L_c = \frac{q_c^*}{r} = \frac{1}{r} \left(\frac{n}{1.49} \right)^9 \frac{g^5}{S_o^{9/2}} \quad (21)$$

From this point of view the flow is everywhere subcritical if $L < L_c$, is mixed if $L > L_c$ and, approaches being everywhere supercritical if $L \gg L_c$.

The typical flow of the mixed condition is sketched in Fig. 4 and for convenience, the relating curves among r , L_c , q_c^* , n , and S_o are plotted in Fig. 5. If any three of the quantities of r , L_c , n , and S_o are known, then the remaining value can be obtained from either Eq. (21) or Fig. 5.

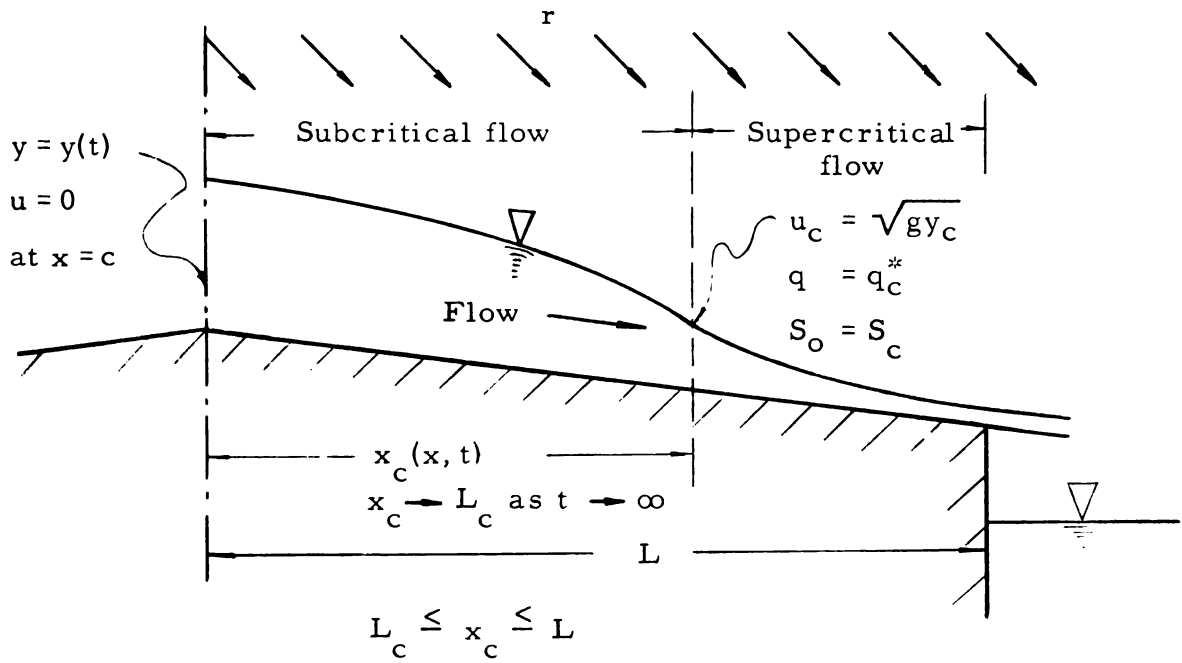


Fig. 4. Sketch of a mixed flow.

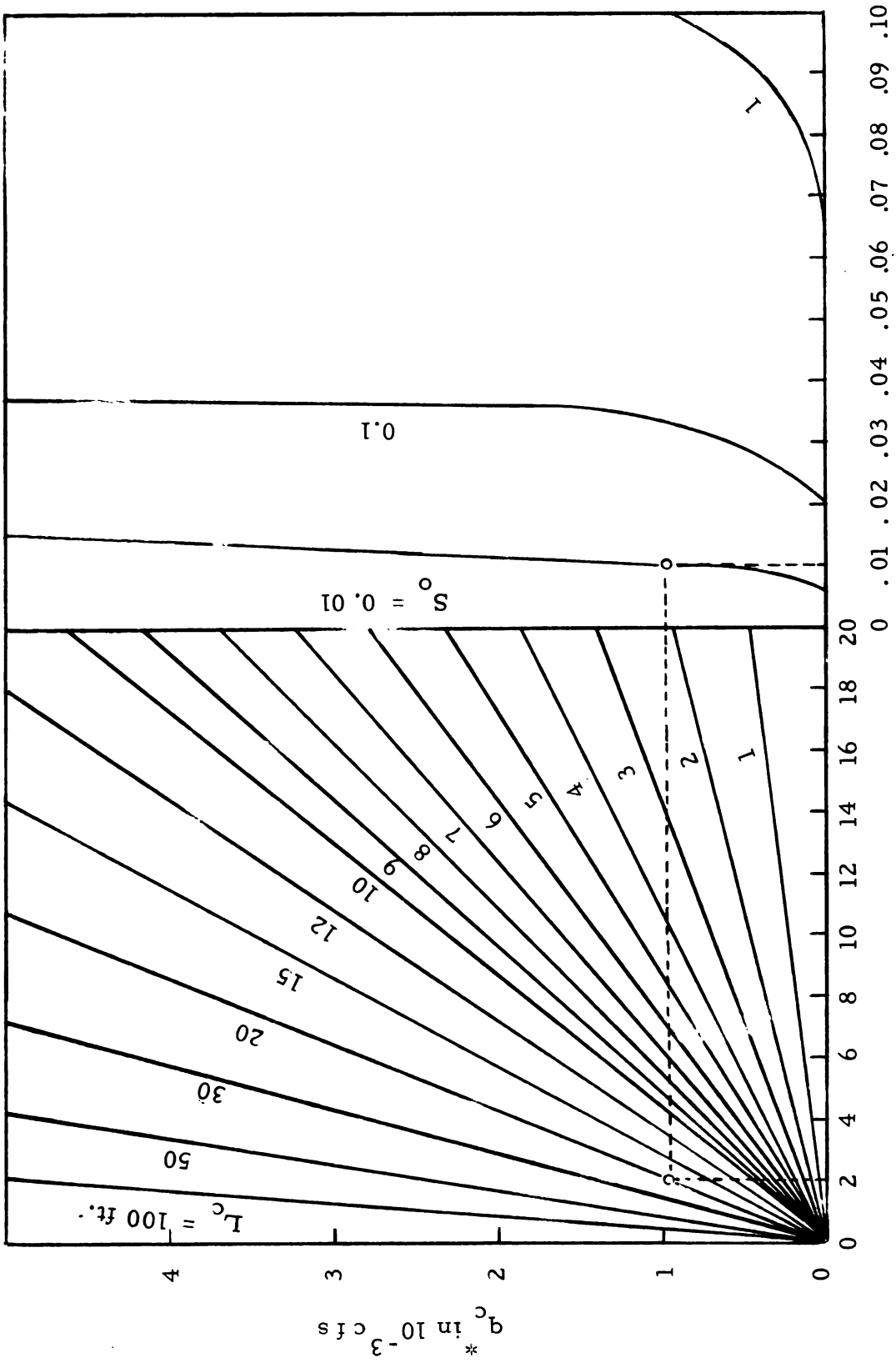


Fig. 5. Relating curves among S_o , n , q_c , r , and L_c .

PROCEDURE OF SOLUTION

Finite-difference scheme. The overland flow problem as posed by Eqs. (3) and (8) with specific initial and boundary conditions is the propagation problem in the continuous system in which solutions are desired for the two dependent variables y and u as functions of the two independent variables x and t . The solution domain has an open shape, therefore, initial or boundary conditions are specified along the open boundary and the governing set of partial differential equations must be satisfied within the solution domain.

Solving Eqs. (3) and (8) simultaneously for $\frac{\partial y}{\partial x}$, gives

$$\frac{\partial y}{\partial x} = \frac{1}{g(y+\xi) - \beta u^2} \left[g(S_o - S_f)y + (v \tan \phi - 2\beta u) r + (2\beta - 1)u \frac{\partial y}{\partial t} - y \frac{\partial u}{\partial t} \right] \quad (22)$$

and for $\frac{\partial u}{\partial x}$,

$$\frac{\partial u}{\partial x} = \frac{1}{g(y+\xi) - \beta u^2} \left[-g(S_o - S_f)u - (v \tan \phi - \beta u) \frac{ru}{y} + gr - \left[g + (\beta - 1) \frac{u^2}{y} \right] \frac{\partial y}{\partial t} + u \frac{\partial u}{\partial t} \right] \quad (23)$$

Note that $\frac{\partial y}{\partial x}$ and $\frac{\partial u}{\partial x}$ for the limiting steady-state condition can be obtained by dropping the $\frac{\partial y}{\partial t}$ and $\frac{\partial u}{\partial t}$ terms in Eqs. (22) and (23) since $\frac{\partial y}{\partial t}$ and $\frac{\partial u}{\partial t}$ approach zero as t approaches infinity.

In the finite-difference technique used in this analysis the solution is marched forward on a fixed rectangular grid or network made up of

x_i and t_j lines for i and j equal to 0, 1, 2, The basic computational operation consists in applying recurrence formulas, derived from Eqs. (3) and (22), to obtain solution values at a new point from previously obtained values. A single application of the recurrence formulas equates a linear combination of four unknown values in the $j + 1$ row to a linear combination of four known values in the j row. A pair of recurrence formulas derived from Eqs. (3) and (22) may be written as follows:

$$u_{i+1,j+1} = \frac{1}{y_{i+1,j+1}} \left[(2r \Delta x + u_{i,j} y_{i,j} + u_{i,j+1} y_{i,j+1} - u_{i+1,j} y_{i+1,j}) - \frac{\Delta x}{\Delta t} (y_{i,j+1} - y_{i,j} + y_{i+1,j+1} - y_{i+1,j}) \right] \quad (24)$$

$$y_{i+1,j+1} = y_{i,j+1} + \frac{\Delta x}{q(y_{i,j+1} + \xi) - \beta(u_{i,j+1})^2} \left\{ \left[g S_o - g \left(\frac{n}{1.49} \right)^2 \frac{(u_{i,j+1})^2}{4/3} \right] y_{i,j+1} + (v \tan \phi - 2\beta u_{i,j+1}) r + (2\beta - 1) u_{i,j+1} \left[\frac{y_{i,j+1} - y_{i,j}}{\Delta t} \right] - y_{i,j+1} \left[\frac{u_{i,j+1} - u_{i,j}}{\Delta t} \right] \right\} \quad (25)$$

for $i = 0, 1, 2, \dots, n - 1$.

and $j = 0, 1, 2, \dots$

where the subscript i, j denotes the upstream section at $t_j = j\Delta t$; the

subscript $i, j+1$ the upstream section at $t_{j+1} = (j+1)\Delta t$; the subscript $i+1, j$ the downstream section at t_j ; and the subscript $i+1, j+1$ the downstream section at t_{j+1} .

The initial and boundary conditions for the subcritical case are

$$y_{i,0} = 0 \text{ and } u_{i,0} = 0 \text{ for } i = 0, 1, 2, \dots, n-1$$

$$u_{0,j} = 0 \text{ and } u_{n,j} = \sqrt{gy_{n,j}} \text{ for } j = 0, 1, 2, \dots$$

Note that theoretically at the critical section, the slope of water surface must be infinite so that the denominator of Eq. (25) must be set to zero, that is

$$g(y_{n,j} + \xi) - (u_{n,j})^2 = 0 \text{ for } j = 0, 1, 2, \dots$$

Hence, a better approximation of the criterion for critical flow would be

$$u_{n,j} = \sqrt{g(y_{n,j} + \xi)/\beta} \text{ for } j = 0, 1, 2, \dots$$

The definition sketches are shown as in Figs. 6 and 7.

Equations (24) and (25) with the given boundary condition at the critical section form implicitly a set of $2n+1$ simultaneous equations when $0, 1, 2, \dots, n-1$ are substituted in the subscript i . There are $2n+2$ unknowns in this set of equations, but since $u_{0,j+1} = 0$ is known, there remains only $2n+1$ unknown values in the $j+1$ row presuming all values in the j row are known from the previous computation.

Thus, in general, starting at any time $t = t_j$ with known values

$y_{i,j}$, $u_{i,j}$, $y_{i+1,j}$, and $u_{i+1,j}$, the values of $y_{i,j+1}$, $u_{i,j+1}$,

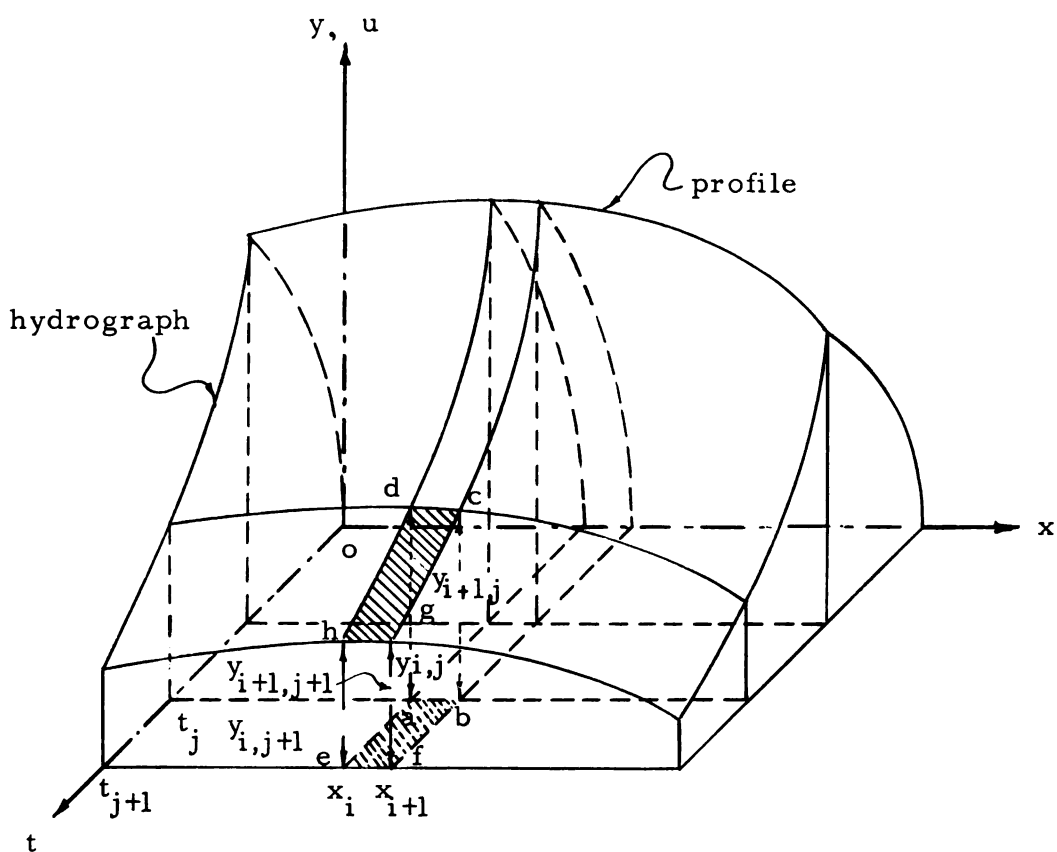


Fig. 6. The solution surfaces in the x - t - y and x - t - u spaces cut by 4 planes $x = x_i$, $x = x_{i+1}$, $t = t_j$, and $t = t_{j+1}$.

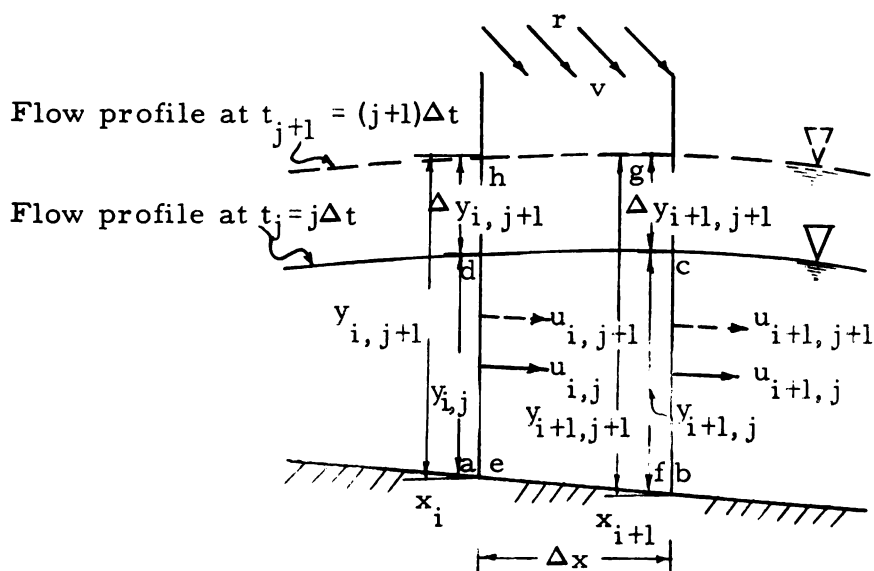


Fig. 7. Definition sketch for the method of finite difference.

$y_{i+1,j+1}'$ and $u_{i+1,j+1}$ could be determined by simultaneously solving the set of $2n+1$ recurrence formulas. However, the easiest way to solve this set of equations is to assume a value of $y_{o,j+1}$ and then methodically correct the assumed value until the boundary condition at the critical section is satisfied; the repetitious computations being performed by a digital computer.

Digital computer routines. In Eqs. (24) and (25), if $y_{o,j+1}$ can be determined, then $y_{1,j+1}'$, $u_{1,j+1}$, $y_{2,j+1}'$, $u_{2,j+1}$, \dots , $y_{n,j+1}'$, $u_{n,j+1}$ can be solved by successive application of Eqs. (24) and (25). A trial-and-error method is introduced to determine $y_{o,j+1}$. It is readily apparent that $y_{o,j+1}$ will be between $y_{o,j}$ and $y_{o,j} + r\Delta t$, therefore, it can be written as

$$y_{o,j+1} = y_{o,j} + [c_1(1/2)r\Delta t + c_2(1/2)^2 r\Delta t + \dots + c_k(1/2)^k r\Delta t] \quad (26)$$

where the coefficients c_1, c_2, \dots, c_k can be either 1 or 0 depending on the boundary value of the downstream end obtained from successive substitution of $y_{i,j+1}$ and $u_{i,j+1}$ in Eqs. (24) and (25). The value of k in Eq. (26) should be taken large enough to assure, within the required accuracy,

$$r\Delta t = c_1(1/2)r\Delta t + c_2(1/2)^2 r\Delta t + \dots + c_k(1/2)^k r\Delta t$$

if c_1, c_2, \dots, c_k are all assumed one.

Values for $y_{o,j+1}$ for successive trials are obtained as follows:

$$y_{o,j+1}^{(1)} = y_{o,j} + c_1 (1/2)r\Delta t$$

$$y_{o,j+1}^{(2)} = y_{o,j} + c_1(1/2)r\Delta t + c_2(1/2)^2 r\Delta t$$

.

$$y_{o,j+1}^{(k)} = y_{o,j} + c_1(1/2)r\Delta t + c_2(1/2)^2 r\Delta t + \dots + c_k(1/2)^k r\Delta t$$

Then, for the first trial, we take $y_{o,j+1}^{(1)}$ with $c_1 = 1$ and check how $y_{n,j+1}^{(1)}$ satisfies the boundary condition

$$u_{n,j+1} = \sqrt{gy_{n,j+1}} \quad (27)$$

If it does not, then $y_{o,j+1}^{(2)}$ is tried, then $y_{o,j+1}^{(3)}$, etc. until the boundary condition is satisfied with prescribed precision. Once $y_{o,j+1}$ is determined, values of y and u for each section x_i will also have been computed.

The generalized computer routine was arranged in such a way that a satisfactory value of $y_{o,j+1}$ could be reached for both subcritical and mixed flows. Presuming the value of $y_{o,j+1}^{(m)}$ for the m th trial.

$$y_{o,j+1}^{(m)} = y_{o,j} + c_1(1/2)r\Delta t + c_2(1/2)^2 r\Delta t + \dots + c_{m-1}(1/2)^{m-1} r\Delta t + c_m(1/2)^m r\Delta t$$

if c_1, c_2, \dots, c_{m-1} are all known (either 0 or 1) from the 1st, 2nd, . . . ,

and (m-1)th trials of $y_{o,j+1}$. Then, to determine the value of c_m (0 or 1), as a rule, the following conditions must be checked at every section x_i , namely,

$$u_{i,j+1} \begin{matrix} > \\ \approx \\ < \end{matrix} \sqrt{gy_{i,j+1}} \quad (28)$$

$$q_{i,j+1} \begin{matrix} > \\ \approx \\ < \end{matrix} q_c^* \quad (29)$$

Five possible cases can be encountered during the computation.

Case I. If $u_{i,j+1}^{(m)} < \sqrt{gy_{i,j+1}^{(m)}}$, then the computation will continue until the downstream end is reached except,

I-1. if $y_{i,j+1}^{(m)} < 0$, the assumed value of $y_{o,j+1}$ was far smaller than the correct one, therefore, $c_m = 1$ and $y_{c,j+1}$ is reassumed.

I-2. if $y_{i,j+1}^{(m)} > y_{i,j} + r\Delta t$, the assumed value of $y_{o,j+1}$ was far larger than the correct one, therefore, $c_m = 0$ and $y_{o,j+1}$ is reassumed.

I-3. if neither I-1 or I-2 and at the overfall $u_{n,j+1}^{(m)} < \sqrt{gy_{n,j+1}^{(m)}}$, the assumed value of $y_{o,j+1}$ was apparently too large, therefore, $c_m = 0$ and $y_{o,j+1}$ is reassumed.

Case II. If $u_{i,j+1}^{(m)} > \sqrt{gy_{i,j+1}^{(m)}}$ one should check Eq. (29) for a mixed flow, and

II-1. if $q_{i,j+1}^{(m)} < q_c^*$, then the flow could be subcritical or a mixed flow with the assumed value of $y_{o,j+1}$ too small, therefore, $c_m = 1$ and $y_{o,j+1}$ is reassumed.

II-2. if $q_{i,j+1}^{(m)} > q_c^*$, then the flow should be a mixed. It is apparent that the assumed value of $y_{o,j+1}$ was too large to meet exactly two conditions, at the critical section,

$$u_{i,j+1} = \sqrt{gy_{i,j+1}} \quad (30)$$

and

$$q_{i,j+1} = q_c^* \quad (31)$$

therefore, $c_m = 0$ and $y_{o,j+1}$ is reassumed.

For illustration, as shown in Fig. 8, a depth of \overline{oa} is assumed for the first trial.

$$\overline{oa} = y_{o,j+1}^{(1)} = y_{o,j} + (1/2)r\Delta t$$

But the resulting profile curve \overline{ab} as shown in the figure is not satisfactory (Case I-1) and it is apparent that \overline{oa} is too small a depth. For the next trial a depth of \overline{oc} is tried.

$$\overline{oc} = y_{o,j+1}^{(2)} = y_{o,j} + (1/2)r\Delta t + (1/2)^2 r\Delta t$$

The resulting profile curve \overline{cd} is not satisfactory either (Case I-2), and \overline{oc} is obviously too large. Using a depth \overline{oe} in the next trial,

$$\overline{oe} = y_{o,j+1}^{(3)} = y_{o,j} + (1/2)r\Delta t + (1/2)^3 r\Delta t$$

The resulting profile curve \overline{ef} is slightly shallow (Case II-1), hence \overline{og} is assumed as the depth for the fourth trial.

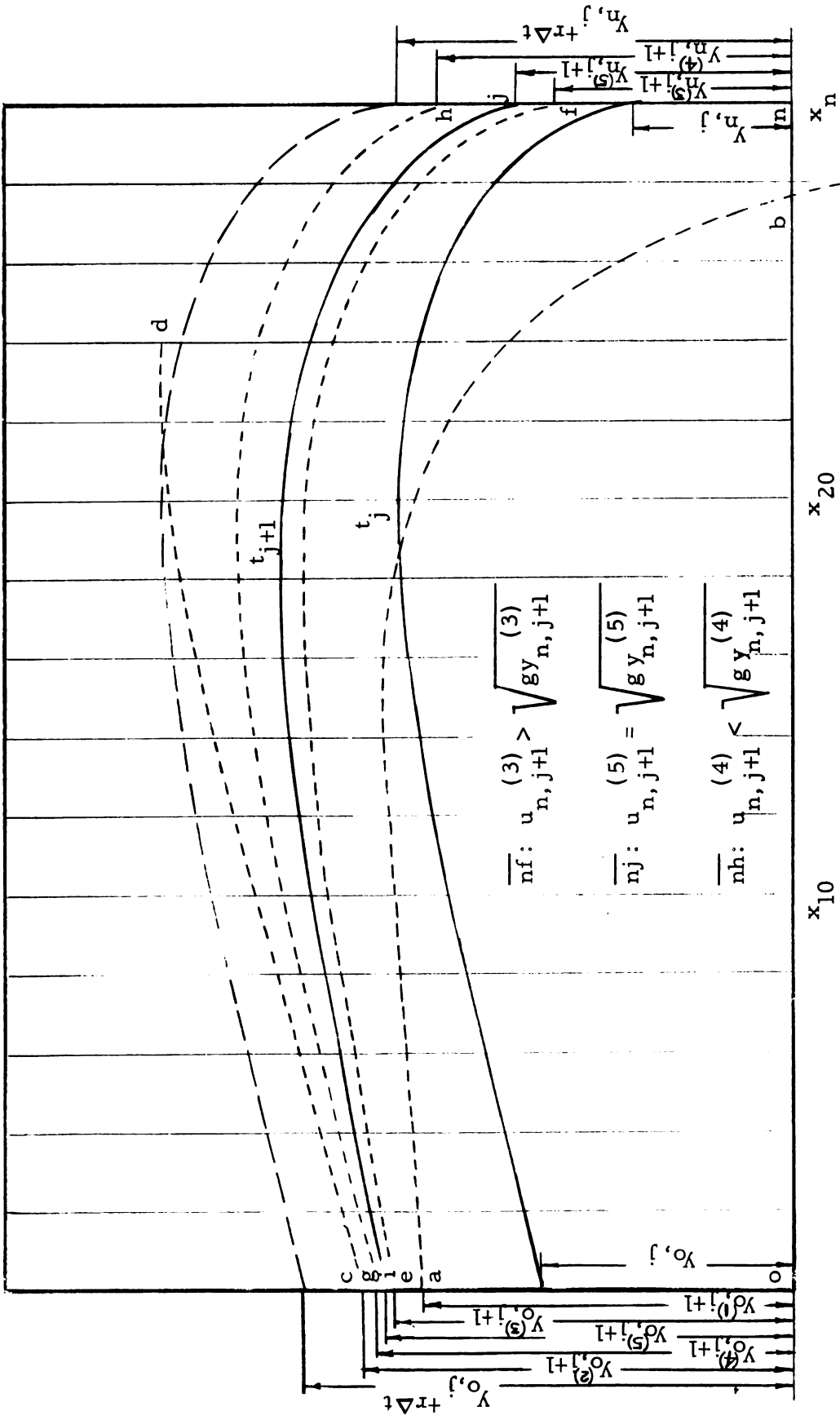


Fig. 8. Sketch of flow profile determined by trial-and-error method.

$$\overline{og} = y_{o,j+1}^{(4)} = y_{o,j} + (1/2)r\Delta t + (1/2)^3 r\Delta t + (1/2)^4 r\Delta t$$

The resulting profile curve \overline{gh} is high (Case I-3) and for the fifth trial \overline{oi} is taken as the depth.

$$\overline{oi} = y_{o,j+1}^{(5)} = y_{o,j} + (1/2)r\Delta t + (1/2)^3 r\Delta t + (1/2)^5 r\Delta t$$

The resulting profile curve \overline{ij} is finally close enough. Note that in the final equation of $y_{o,j+1}$, $c_1 = c_3 = c_5 = 1$ and $c_2 = c_4 = 0$, and that the exact solution can be approached as closely as desired. In the case of mixed flow, Cases II-1 and II-2 are used not only to determine the value of $y_{o,j+1}$ but also to obtain approximately the position of the critical section at t_{j+1} .

For the recession stage of overland flow, since $r = 0$ an assumption scheme similar to Eq. (26) is necessary.

$$y_{o,j+1} = c_1(1/2)y_{o,j} + c_2(1/2)^2 y_{o,j} + \dots + c_k(1/2)^k y_{o,j} \quad (32)$$

where, in the same manner, c_1, c_2, \dots, c_k will be either 1 or 0.

The procedure otherwise follows the same pattern as described before.

RESULTS AND DISCUSSION

A total of eight computations were made with the flow in the sub-critical regime. In the first run the surface was horizontal with a length of 30 feet and an n value of 0.01, and the rainfall was vertical at 2 inches per hour. In each of the subsequent runs one factor was changed in order to assess its effect -- the values being as shown in Table 1. A Δx of 1 foot and a Δt of 10 seconds were used in all the computations.

Table 1. Subcritical runs.

Factor	Run 1	Run 2	Run 3	Run 4	Run 5	Run 6	Run 7	Run 8
n	0.01	0.1	0.01	0.01	0.01	0.01	0.01	0
S_o	0	0	0.001	0	0	0	0	0
L ft	30	30	60	30	30	30	30	30
r in/hr	2	2	2	2	20	2	2	2
ϕ degree	0	0	0	0	0	+45	-45	0

For illustration, the whole scheme of results of Run 5 is presented to show the completeness of the picture obtainable from the computational procedure. Figures 9, 10, and 11 show the variation of depth with respect to distance and time, Figs. 12, 13, and 14 the variation

of velocity with respect to distance and time, and Figs. 15, 16 and 17 the variation of discharge with respect to distance and time.

Figures 9 and 10 show the profiles of water depth, with time as a parameter, during and after rainfall. At the beginning of rainfall the profile is very flat for almost the entire length of the channel suddenly dropping near the overfall. As time goes on, the effect of the downstream control is increasingly noticeable upstream and the profile becomes steeper approaching the limit of the steady state. At the beginning the phenomenon is primarily one of storage; the rate of increase of depth being almost equal to the rate of rainfall. At the steady state limit, of course, no more storage is possible. Figure 11 shows the stage-hydrographs for different positions on the slope. All of the rising limbs are asymptotic to a straight line corresponding to the rate of rainfall and to horizontal asymptotes corresponding to the steady state. On the falling stage, if the discharge were to continue to be a straight line variation with distance (as it is at the steady state and almost is at 330 seconds), then the depth would have to decrease at the same rate everywhere, since release from storage is the only source of discharge. That the profile becomes flatter with time is readily apparent in Fig. 10, and that the decrease in depth over a given time is greater for upstream than for downstream sections is emphasized in Fig. 11. The initial condition for the receding stage

was taken as the profile at the cessation of rainfall; the limit is zero flow and zero depth everywhere.

Figures 12 and 13 show the profiles of the mean-velocity along the surface, with time as a parameter, during and after rainfall. The two families of curves appear very similar; the velocity for each curve being zero at the upstream end and increasing in a concave upward curve to a maximum value at the overfall where the partial derivative of velocity with respect to distance is theoretically infinite as indicated by Eq. (23). Figure 14 shows the velocity-hydrographs with distance as a parameter. It is interesting to note that there seems to be an abrupt increase in velocity everywhere at the moment of cessation of rainfall, though the magnitude of the change is different for different x . The conditions on the rising stage at the time the rainfall ceased were assumed to be the condition at the beginning of the recession. For some of the upstream sections, the computed velocity was greater 10 seconds after the rain ceased than at the moment of cessation. Extrapolating the recession curves back, an increase in velocity would be indicated at all stations except at the beginning of the surface where the velocity is always zero and possibly at the overfall where the velocity is always critical. There are several ways in which the rainfall enters the equations describing the flow; continuity, acceleration of the rain to the velocity of the ambient flow, the vertical pressure distribution (or ξ

value), and in the resistance to flow (or n value). The relative importance of these various effects could be tested by special computational runs if ever desired. Such runs have not been included in this study because other questions seemed to be of greater importance.

Figures 15 and 16 show the discharge-profiles, with time as a parameter, during rainfall and in the receding stage, respectively. The discharge, of course, is the product of the depth times the velocity, and the curves, therefore, combine the curves of the appropriate previous figures. During the rainfall, the family of curves describing the discharge are similar to those of the velocity, but the curvature, while still concave upward, is less than for the velocity because the depth curves are concave downward. The discharge profile curve becomes less concave as time goes on and at the steady state limit is a straight line $q = rx$. On the receding stage, the discharge-profile is slightly concave downward but otherwise the family of curves is basically similar to those of the velocity. On the rising stages, Fig. 15, the concave upward curves show that the rate of storage is greater upstream than downstream. On the falling stages, Fig. 16, the concave downward curves show that the release from storage is greater upstream than downstream. Figure 17 shows the discharge-hydrographs for various distances along the surface. Although the discharge 10 seconds after the rain had stopped did not show an increase at any station,

projecting the recession curve back would indicate that shorter time intervals might indicate an increase in discharge immediately after the rain.

In Figs. 18 and 19 the relationships between velocity and depth, and discharge and depth with distance and time as parameters are shown. A network of $x = \text{constant}$ and $t = \text{constant}$ lines in the u - y plane or in the q - y plane describes the complete solution of the overland flow problem. As shown in the figures, the area described by a curve \overline{OA} (downstream boundary condition), a curve \overline{OB} (upstream boundary condition), and a curve \overline{AB} (steady-state condition) forms the domain of the whole solution. The original point 0 is the initial condition where velocity or discharge is zero when the depth equals zero. It is interesting to note that velocity or discharge at any location on the surface during rainfall (solid lines) is less than that after rainfall (dotted lines), except at the overfall where velocity or discharge after rainfall is slightly less than that during rainfall. The control, or critical, criterion differs during and after rainfall by the ξ factor. Since the q - y curves are nonlinear and different on rising and falling stages the assumption of linearity in the method of hydrologic flood routing would not appear to be an acceptable approximation for this problem. In fact, a simple relationship between discharge and stage, or storage, does not appear likely.

The results of the other computations showed basically the same patterns illustrated in Figs. 9-19, and are not, therefore, presented in as great detail. Instead, these results are presented as comparisons to illustrate the effect of the different variable factors.

In Fig. 20, the discharge-hydrographs for a 20-in/hr and a 2-in/hr rain are shown. The time scale for both hydrographs is the same, but the discharge scale is ten times as great for the 20-in/hr rain as for the 2-in/hr rain. Although there is a difference in these two hydrographs, they are sufficiently similar so that they tend to confirm the concept of the unit hydrograph as a workable approximation in real situations. Of the many further calculations that should be made, a series to check unit-hydrograph theory would be among the most interesting.

To test the effect of roughness, n values of 0, 0.01, 0.1 were used with all other factors the same (Runs 8, 1, 2). Figures 21 and 22 show the effect of "roughness" on the discharge-hydrograph and the stage-hydrograph, respectively. It is apparent that the larger the resistance, the more the flow is retarded; this retarding effect is shown in Fig. 22 by the greater depths for larger n , and in Fig. 21 by the greater time required to achieve the same discharge on the rising stage. The same effect, retardation, is shown on the falling stage as the discharge is maintained for a longer period of time (possible because of the greater storage). As shown in Fig. 22, the storage at the steady state on the

"rough" surface is about double that on the "smooth" surfaces. It is interesting to note that if the time scale in Fig. 21 were made dimensionless by using as the unit of time, the time to reach one-half of the steady-state discharges, the discharge hydrographs would collapse almost to a single curve.

The effect of the two surface slopes used ($S_o = 0$ in Run 1, $S_o = 0.001$ in Run 3) on the discharge-hydrograph is very small as shown in Fig. 23. The discharge for $S_o = 0$ is always slightly smaller than that for $S_o = 0.001$ during rainfall, and larger in the receding stage. This effect is similar to that of resistance.

The effect of the slanting rain is also a retardation effect as shown in Fig. 24 where the normal component of the rain, as are all other factors, is kept the same, but the inclination of the rain is vertical (Run 1) or ± 45 degrees from the vertical (positive in Run 6 and negative in Run 7). Within the range of probable values, the retardation effect for the angle and velocity of the raindrops, is probably less than that of roughness, but more than that of slope -- at least for lengths as short as those studied and if only the subcritical flow regime is considered.

In Figs. 25 and 26 the discharge-hydrographs and depth-hydrographs are shown for a station 30 feet from the beginning of the surface where one surface is 30 feet long (Run 1) and the other is 60 feet long

(Run 3). This is equivalent to specifying different controls at 30 feet. At any time on the rising stage, the discharge is less and the depth is greater for the 60 feet surface than for the 30 feet surface -- indicating greater storage as might be expected. It is apparent, however, that the discharge hydrographs would tend to collapse again if the time to reach one-half of the steady state discharge were used as the unit of time.

The possibility of a single approximate overland flow discharge-hydrograph is demonstrated by Figs. 27 and 38. In Fig. 27, the dimensionless discharge at the overfall q/rL is plotted against the dimensionless time $t/t_{1/2}$ for the standard run and for the runs with larger n , larger rainfall, and larger length. The collapse could be improved by using a zero time when one quarter of the discharge is reached and as the unit of time, the time to change from one quarter to three-quarters of the steady stage discharge. This later definition of time might also be preferable for field conditions where the zero time is not conducive to precise interpretation.

Figure 28 is a similar dimensionless plot of discharge q/rx against $t/t_{1/2}$ for $x = 10, 20, 30$ of the standard run, $x = 10, 30$ on the longer surface and $x = 10$ for the larger rainfall and the greater roughness. The fact that the hydrographs for different x do not collapse as well as those for the overfall indicates the importance of the type of

control. However, the collapse of these hydrographs would also be improved by the $t_{1/4}$, $t_{3/4}$ expedients.

One computation was attempted which resulted in the mixed flow condition; all factors being the same except for the slope which had a value of 0.01. The flow was subcritical throughout up to 90 seconds, and the depth profiles, Fig. 29, up to this time are essentially similar to those of Fig. 9. After 90 seconds the control shifted upstream and storage was released downstream from the control although upstream the depth continued to increase slowly.

The full story of the mixed flow could not be depicted in Fig. 29, however, and in Fig. 30 it is seen that the stage hydrograph at the overfall was very erratic after the control shifted upstream -- a discharge hydrograph would display the same behavior. The actual flow may well be unstable, but there is no obvious reason why the real instability should show up in these computations. It is possible that a faster machine permitting the use of a floating-point system in the computation procedure would allow more precision and thereby eliminate the apparent surging. It is also possible that smaller increments of distance and time are required, but again a larger, faster machine would be needed.

The plot of the position of the critical control in Fig. 30 matches the surging at the overfall and leads to the suspicion that the trouble is not the release from and build up of storage in this area, but in the

shifting control itself. A slightly high assumption of the depth at $x = 0$ results in too much storage along the slope, reducing the discharge and thus shifting the control downstream -- similarly a low assumption of the starting depth shifts the control upstream. Therefore, it would seem that more significant figures in the computation are needed. There may be other possible explanations for this erratic behavior, but no obvious errors in the computational procedure have been discovered, and it has been noted that a change in the last significant figure in $y_{o,j}$ can have this sort of effect.

CONCLUSIONS

It would be premature to claim that the analysis of overland flow presented herein is complete, and it would be inaccurate to claim that it is rigorous. It is not complete because the general problem was simplified at the outset, and because the differential equations describing the phenomenon have not been solved except for a few particular sets of conditions. However, the results of those computations that have been made appear to be entirely reasonable, and, with minor modifications of the procedure to take into account such considerations as variable rain and slope, and different controls, more computations should give a rather complete picture of the overland flow problem.

The lack of rigor can be laid to the deficiency in knowledge concerning certain of the subsidiary phenomena; e. g. , the resistance to flow under these conditions of a flow which is not only unsteady and non-uniform but disturbed by the rain penetrating the free surface. The computation procedure, however, provides the means by which the effect and importance of many of these imperfectly known phenomena can be assessed; e. g. , the overpressure due to the normal component of momentum flux of the rain.

The results of the computations which have been made tend to confirm the unit-hydrograph concept. In fact, in the subcritical flow

regime, it would seem that a single dimensionless unit hydrograph could be a practical possibility. Many more computations are needed to confirm this suggestion, especially to extend the range of variables, to include rain variable in time and space, and to assess the effect of controls other than the free overfall. The unit of discharge for such a universal hydrograph (or hydrographs) would obviously be based on the rainfall; but many factors, those already studied and certainly others, must enter into the time base.

Although the problem becomes much larger, requiring a faster, bigger machine for the computations, there seems to be no reason why the attack used here for the overland flow problem cannot be extended to the watershed problem. The real geometry of watersheds would probably be overwhelming, but an investigation of schematic watersheds should provide guidelines to the interpretation of field data by sorting out the effect of the many factors.

REFERENCES

1. Laws, J. O. (1941). Measurements of the fall-velocities of water drops and rain drops. *Trans. Amer. Geophys. Union*, Vol. 22, pp. 709-721.
2. Rouse, Hunter (1949). Engineering Hydraulics. John Wiley and Sons, Inc., New York. 1039 pp.
3. Chow, Ven Te (1959). Open-Channel Hydraulics. McGraw-Hill Book Company, Inc., New York. 680 pp.
4. Izzard, Carl F. (1946). Hydraulics of runoff from developed surfaces. *Proceedings of the 26th Annual Meeting of Highway Research Board*, Vol. 26, pp. 129-146.
5. Iwagaki, Yuichi (1955). Fundamental studies on the run-off analysis by characteristics. *Disaster Prevention Research Institute Bulletin No. 10*, Kyoto University, Kyoto, Japan. 25 pp.
6. Liggett, James A. (1959). Unsteady open channel flow with lateral inflow. Department of Civil Engineering, Stanford University, Stanford, California. Technical Report No. 2. 73 pp.
7. Harder, James A. (1962). Evaluating the basis of computer flood routing. *ASCE Water Resources Engineering Conference*, Omaha, Nebraska. 15 pp.

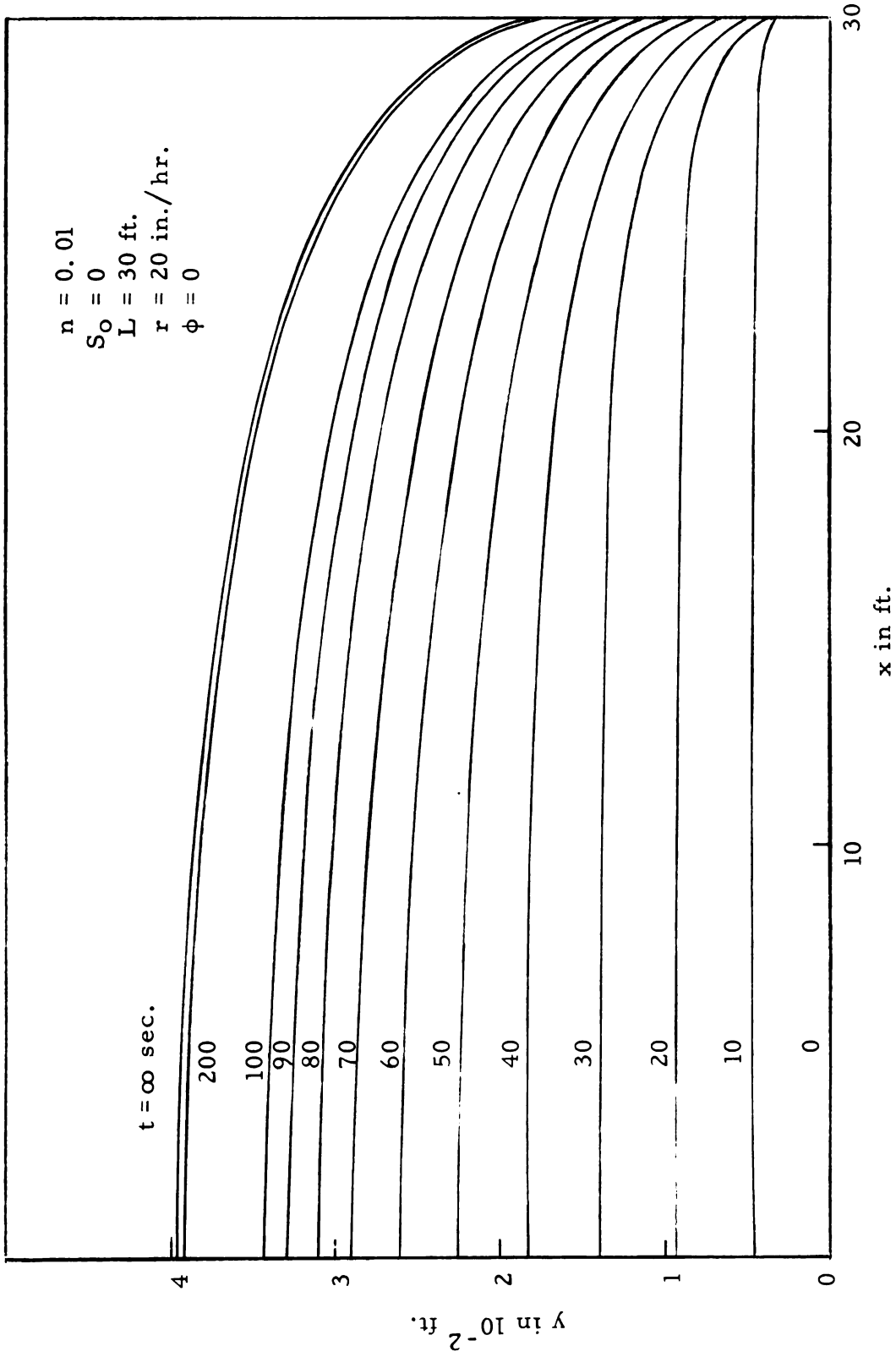


Fig. 9. Profiles of water depth with time as a parameter during rainfall.

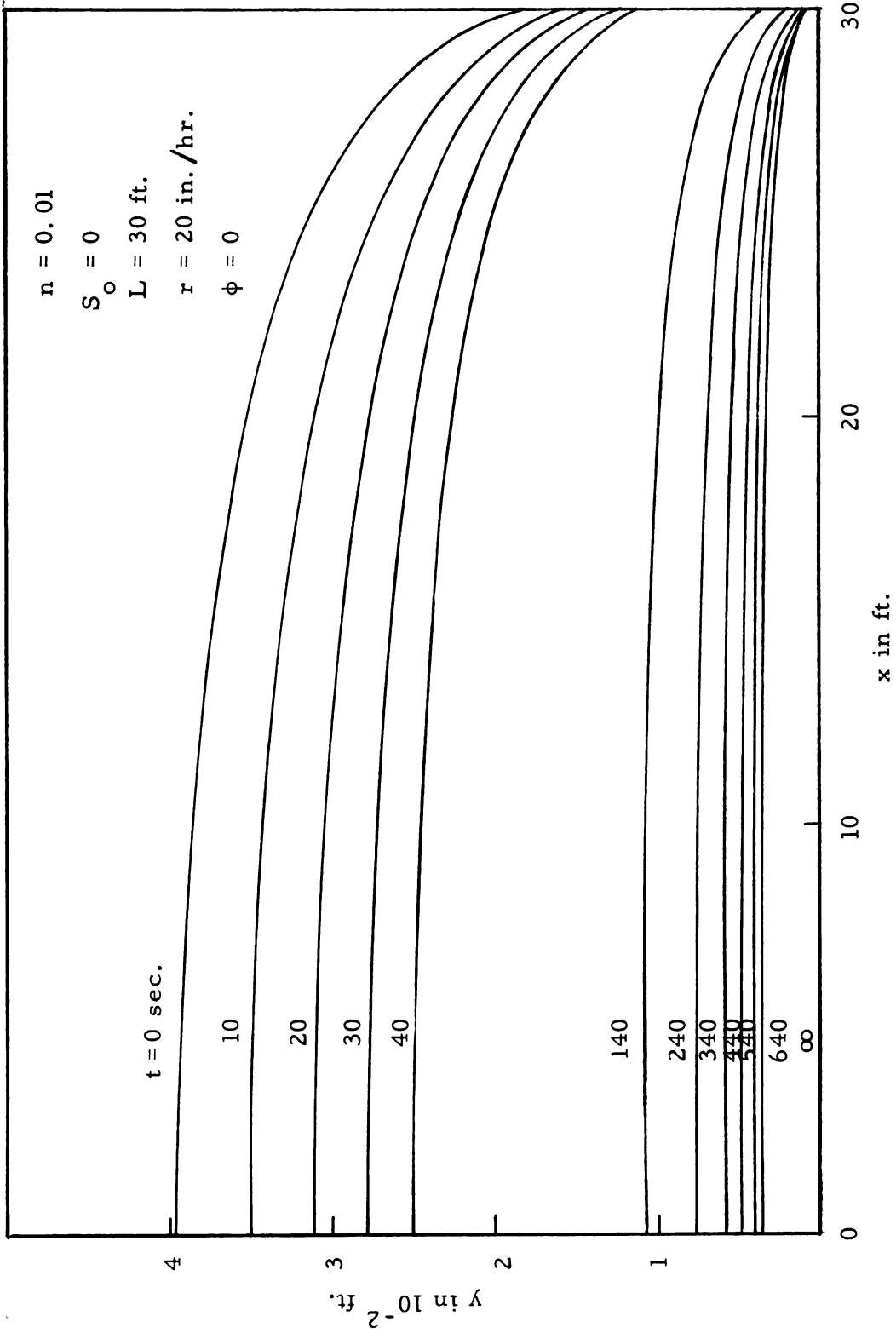


Fig. 10. Profiles of water depth with time as a parameter in the receding stage.

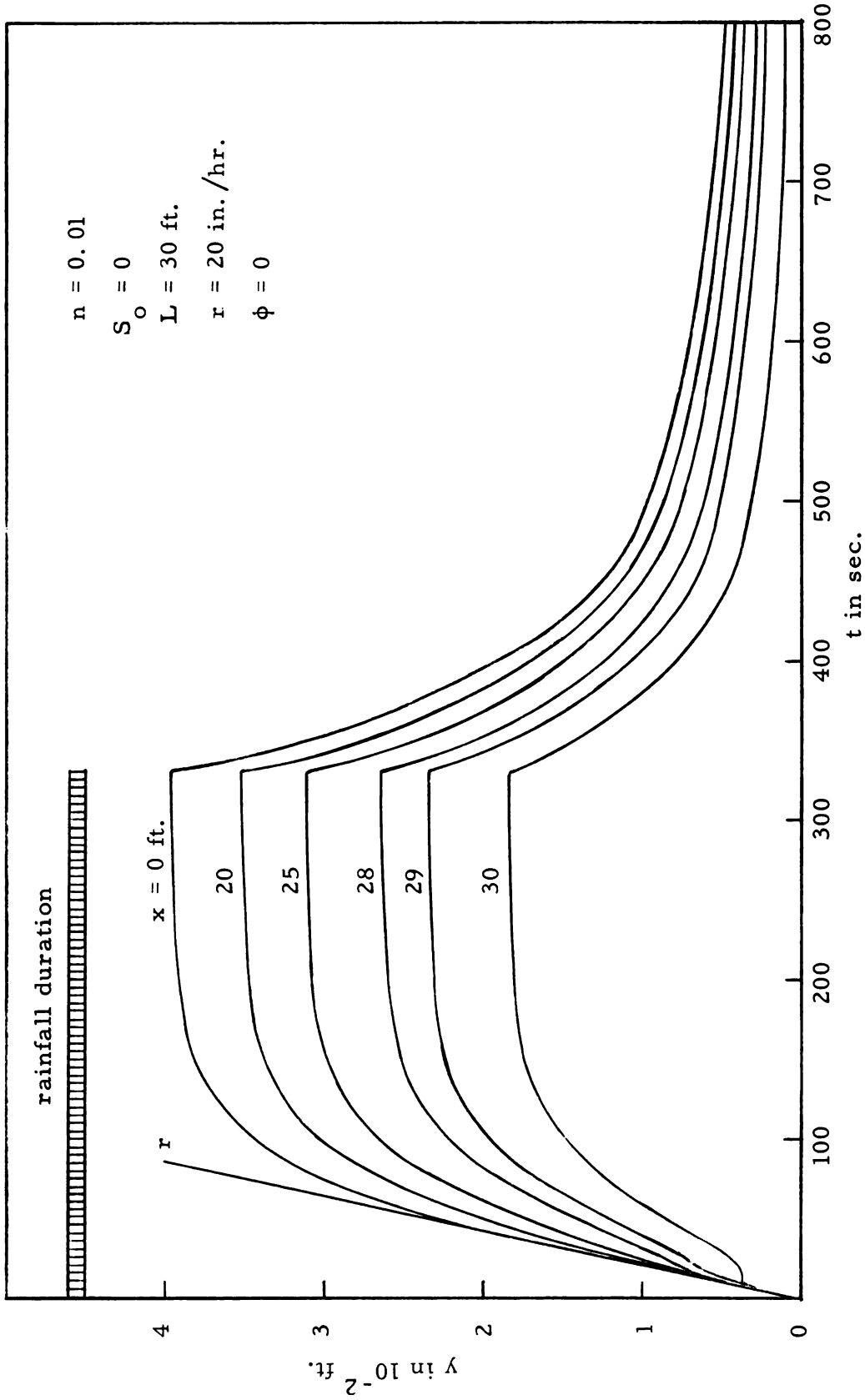


Fig. 11. Stage - hydrographs for different positions on the slope.

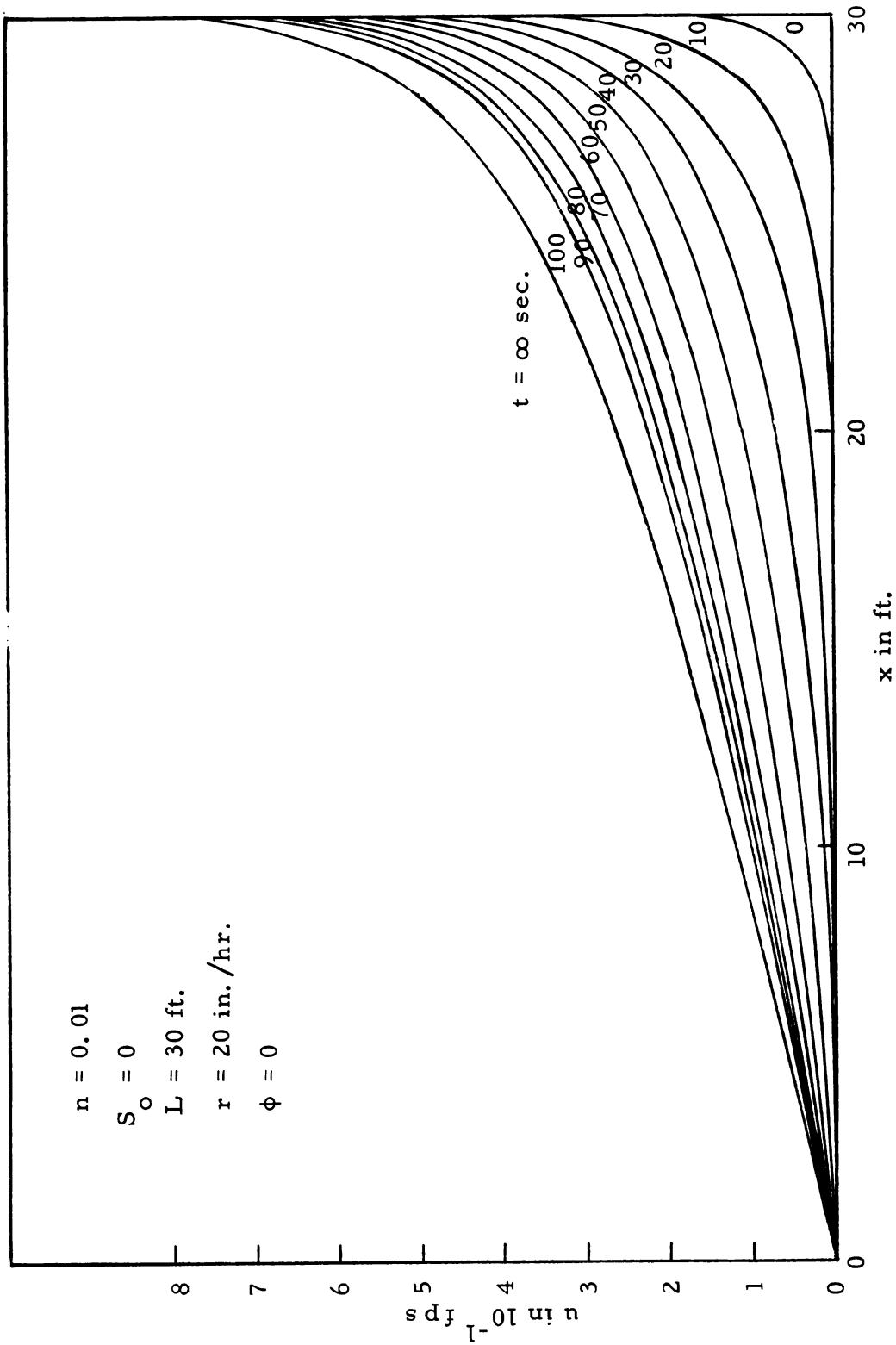


Fig. 12. Profiles of the mean velocity along the surface with time as a parameter during rainfall.

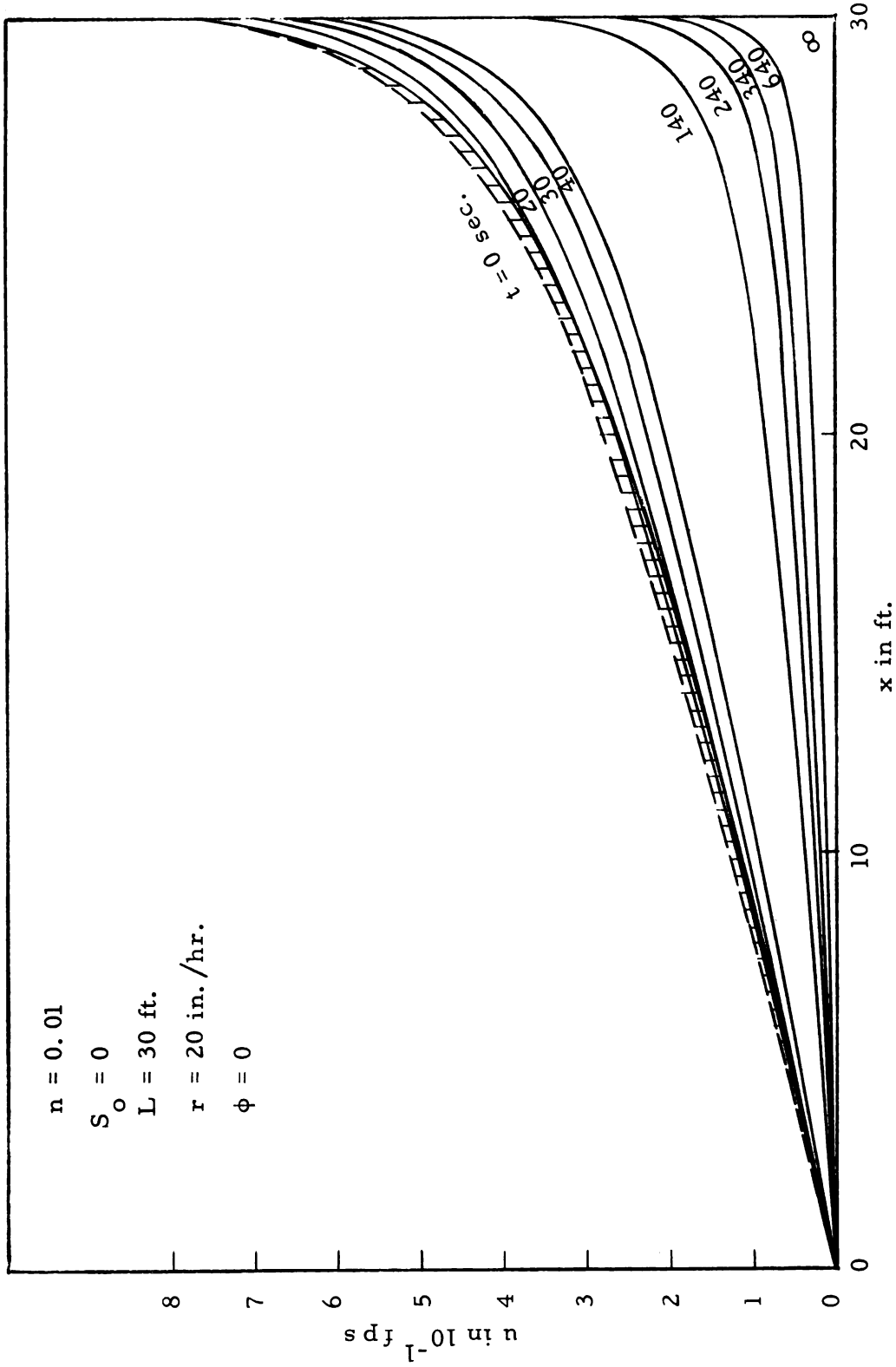


Fig. 13. Profiles of the mean-velocity along the surface with time as a parameter after rainfall.

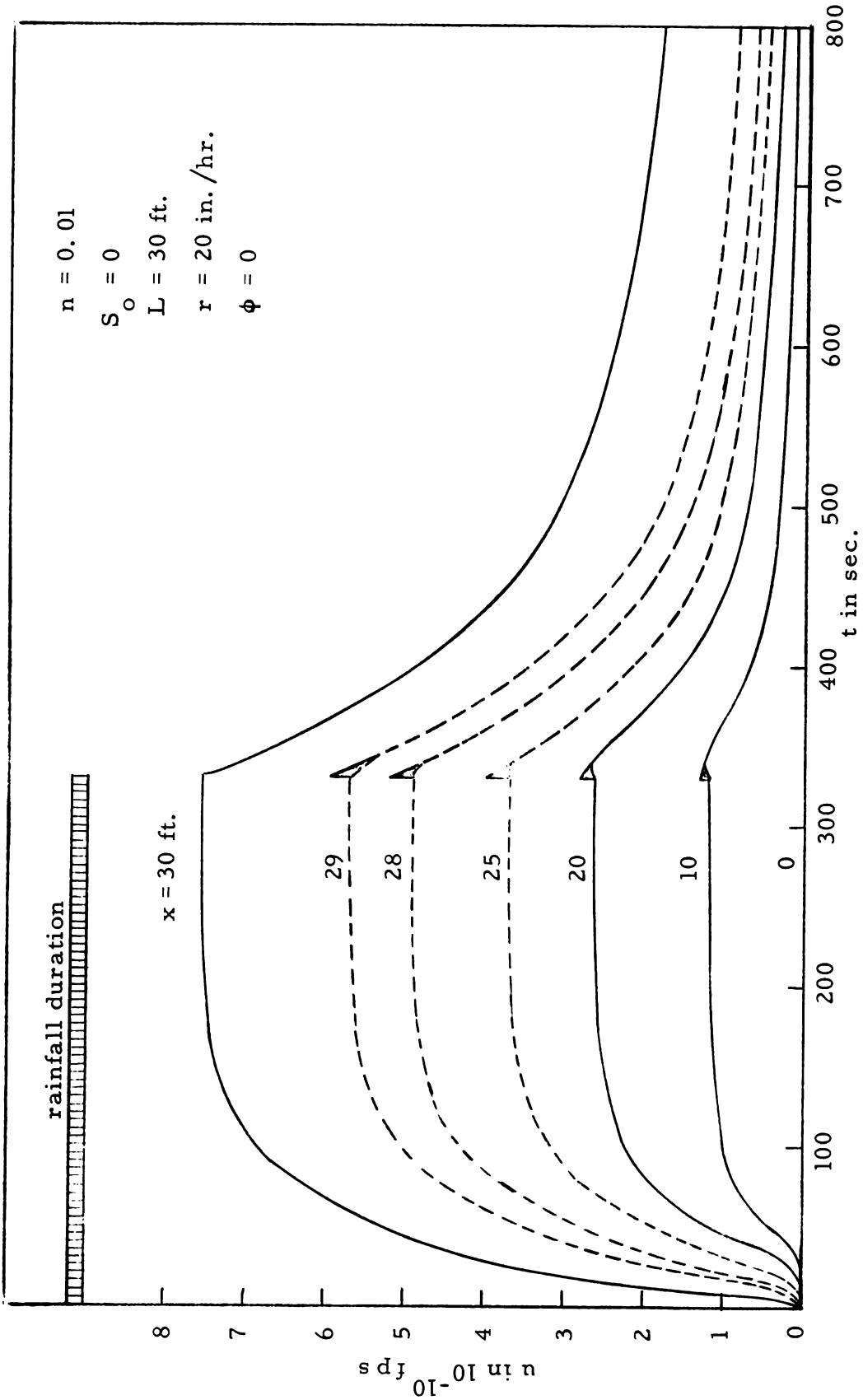


Fig. 14. Velocity-hydrographs with distance as a parameter.

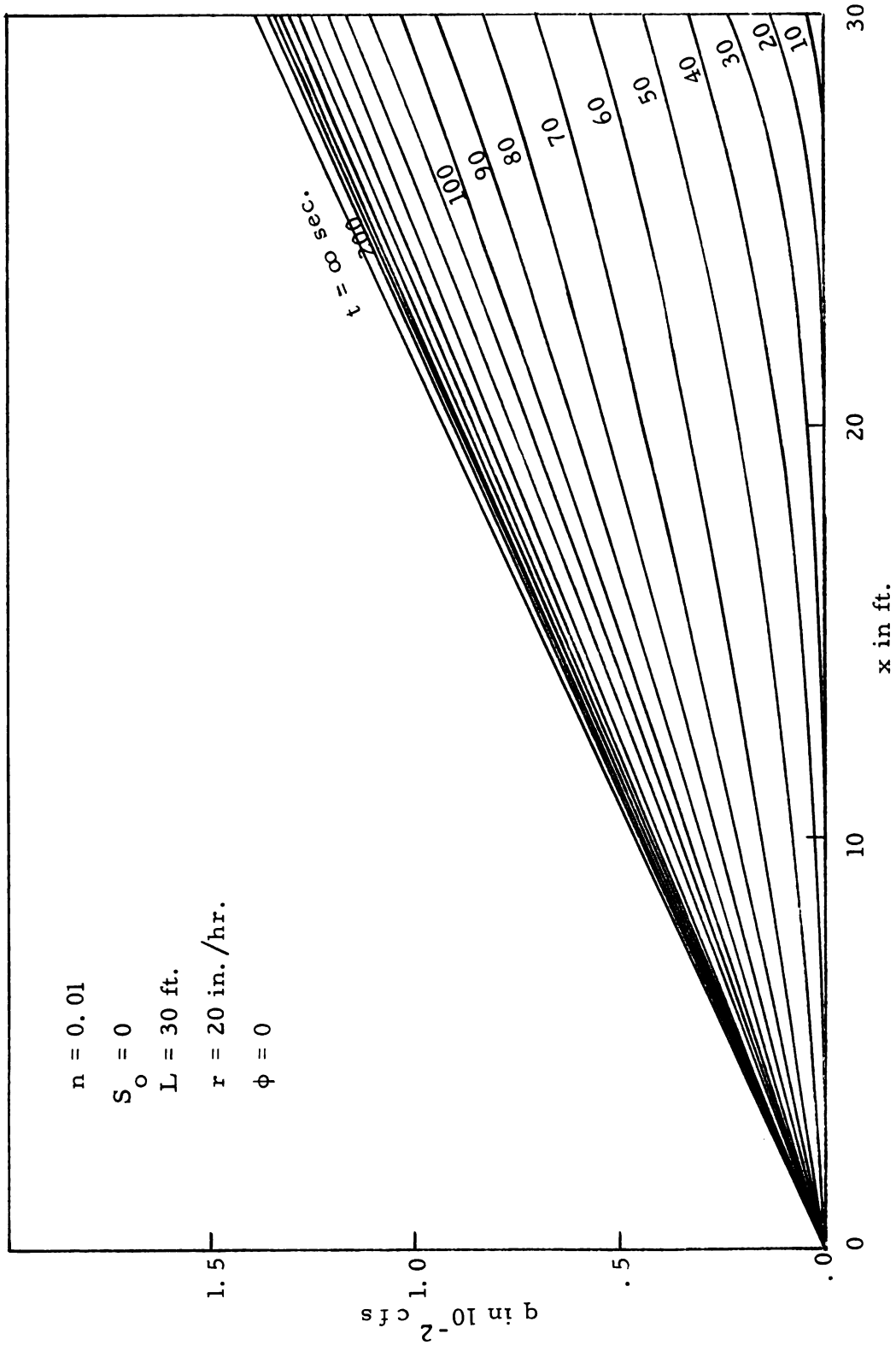


Fig. 15. Discharge - profiles with time as a parameter during rainfall.

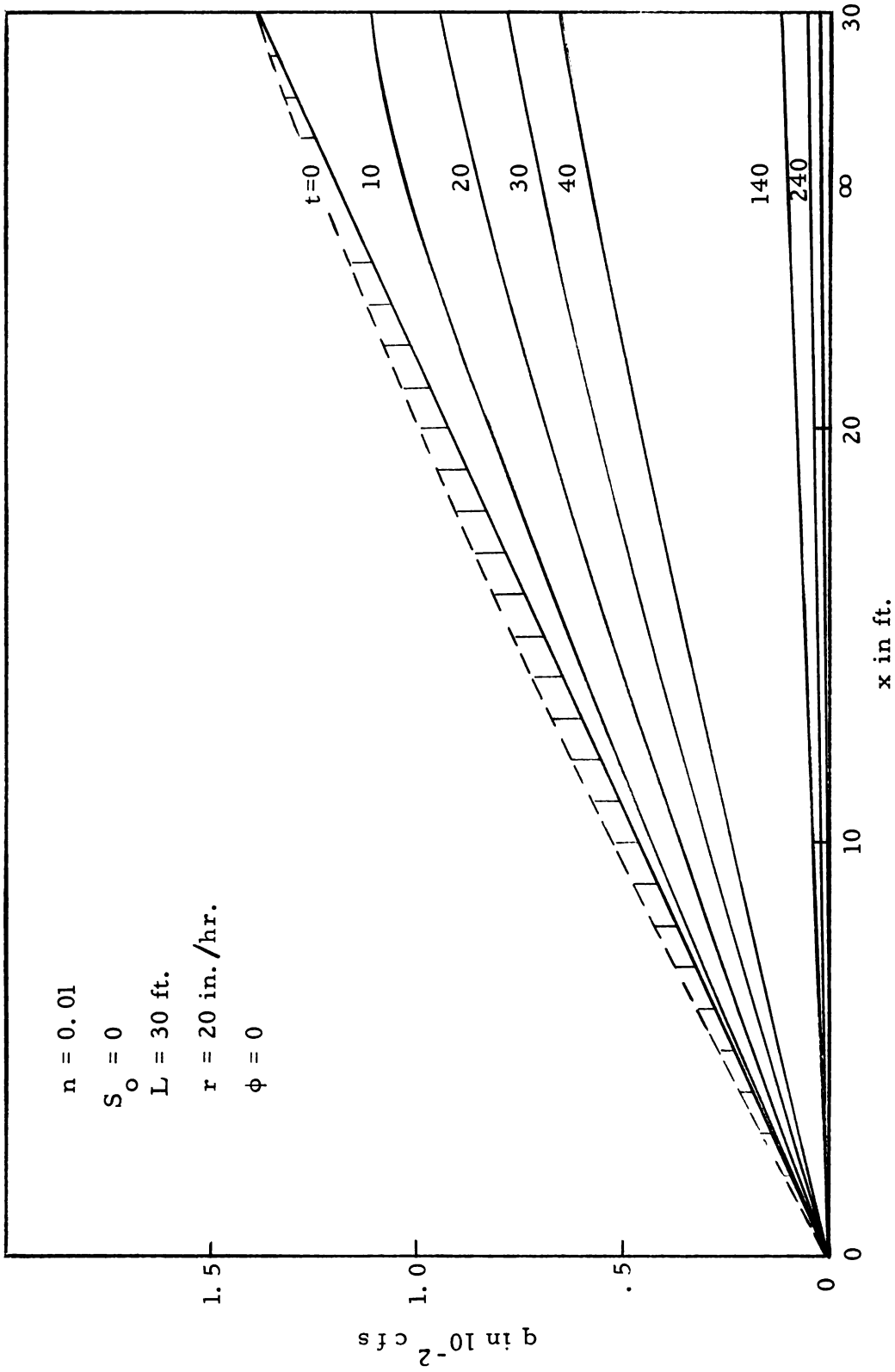


Fig. 16. Discharge - profiles with time as a parameter in the receding stage.

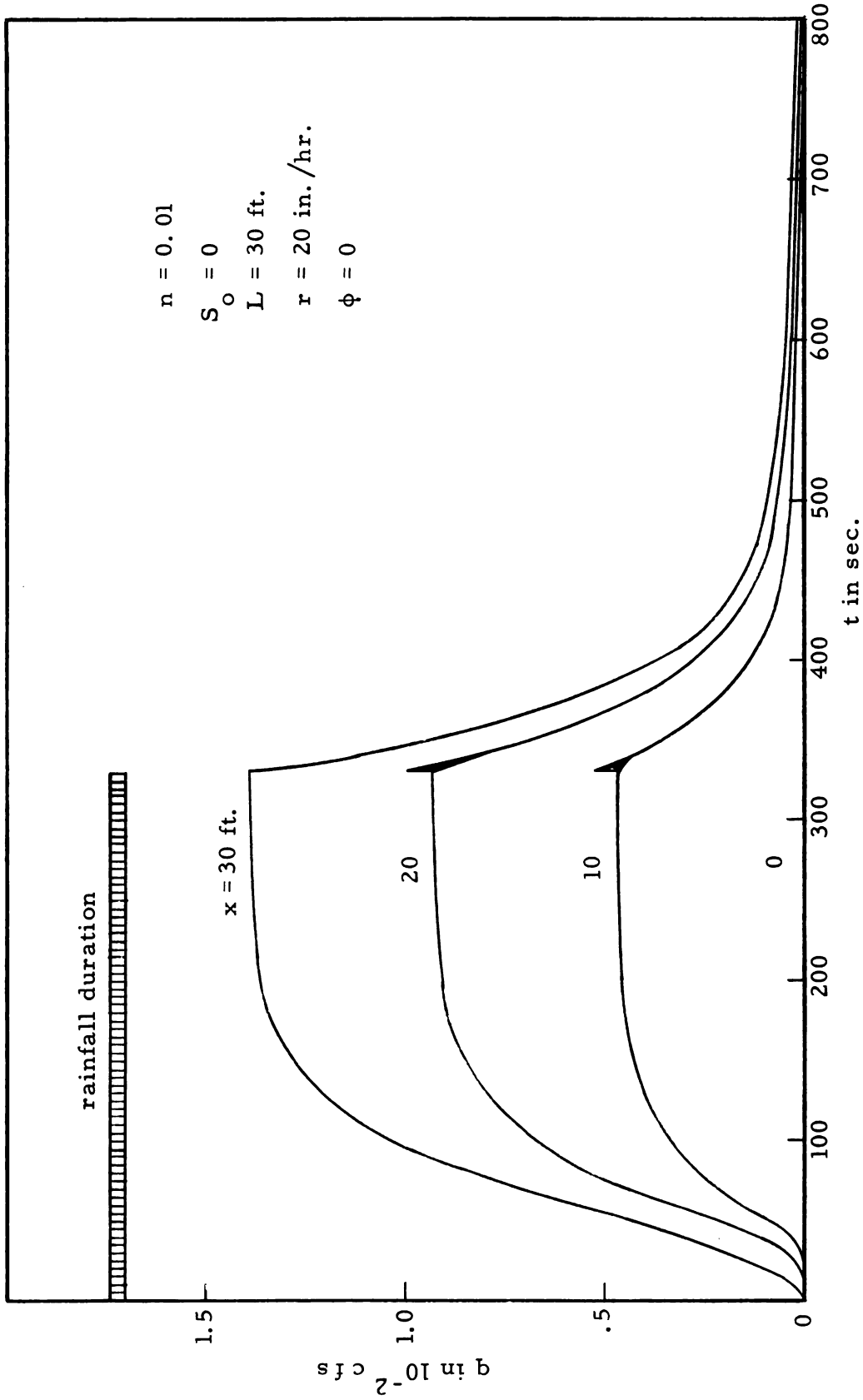


Fig. 17. Discharge - hydrographs for various distances along the surface.

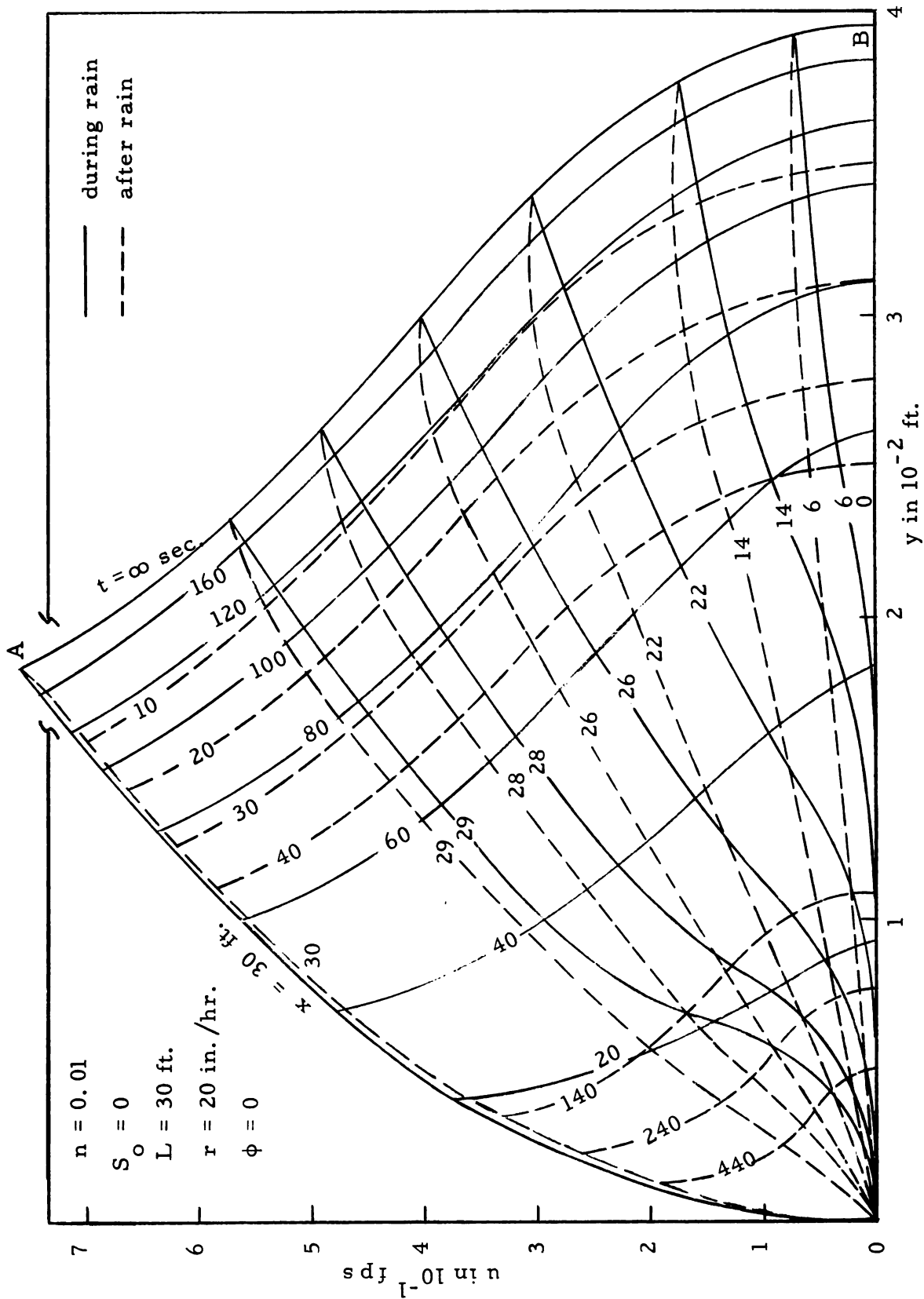


Fig. 18. Relationship between velocity and depth with distance and time as parameters.

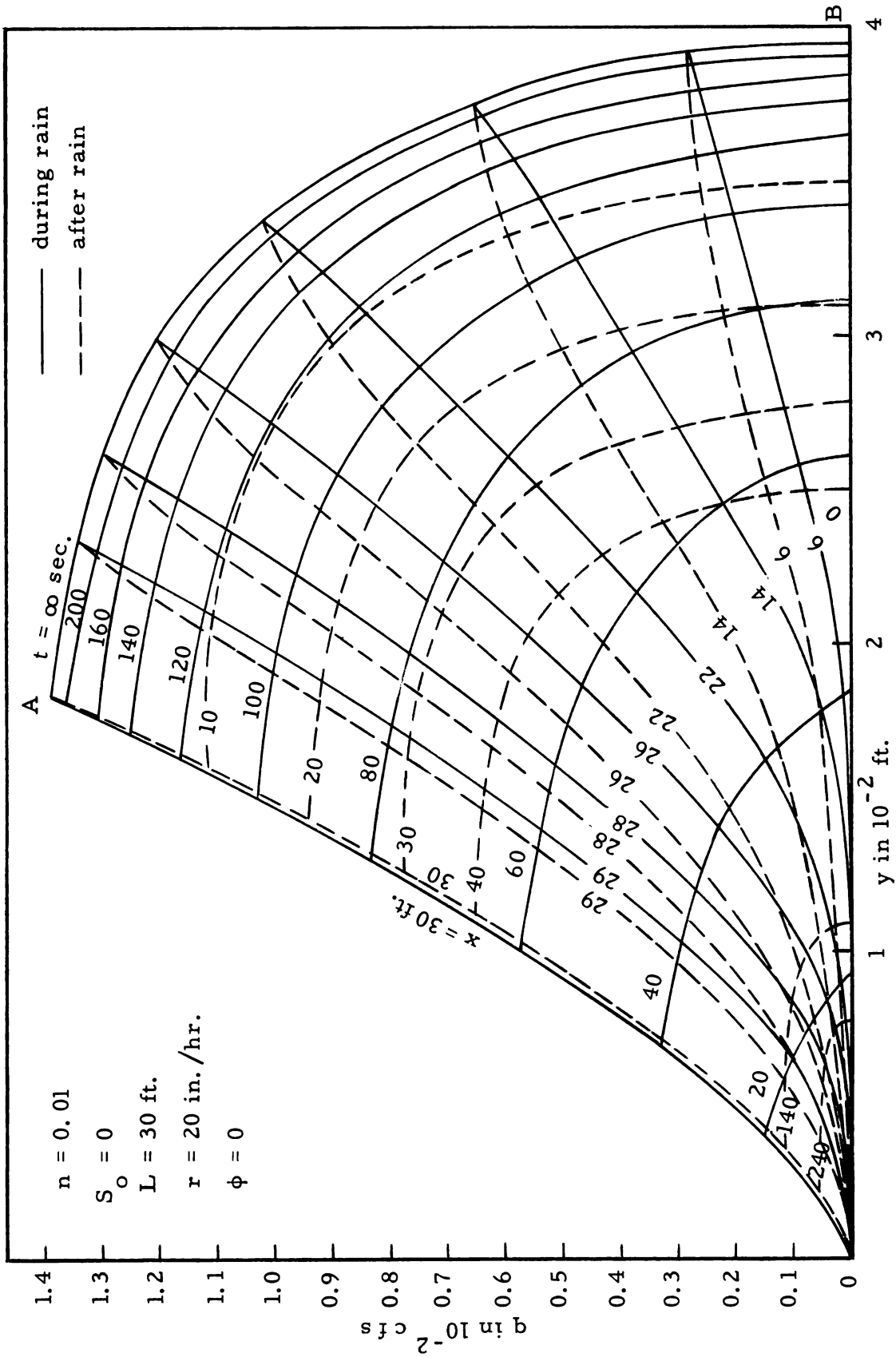


Fig. 19. Relationship between discharge and depth with distance and time as parameters.

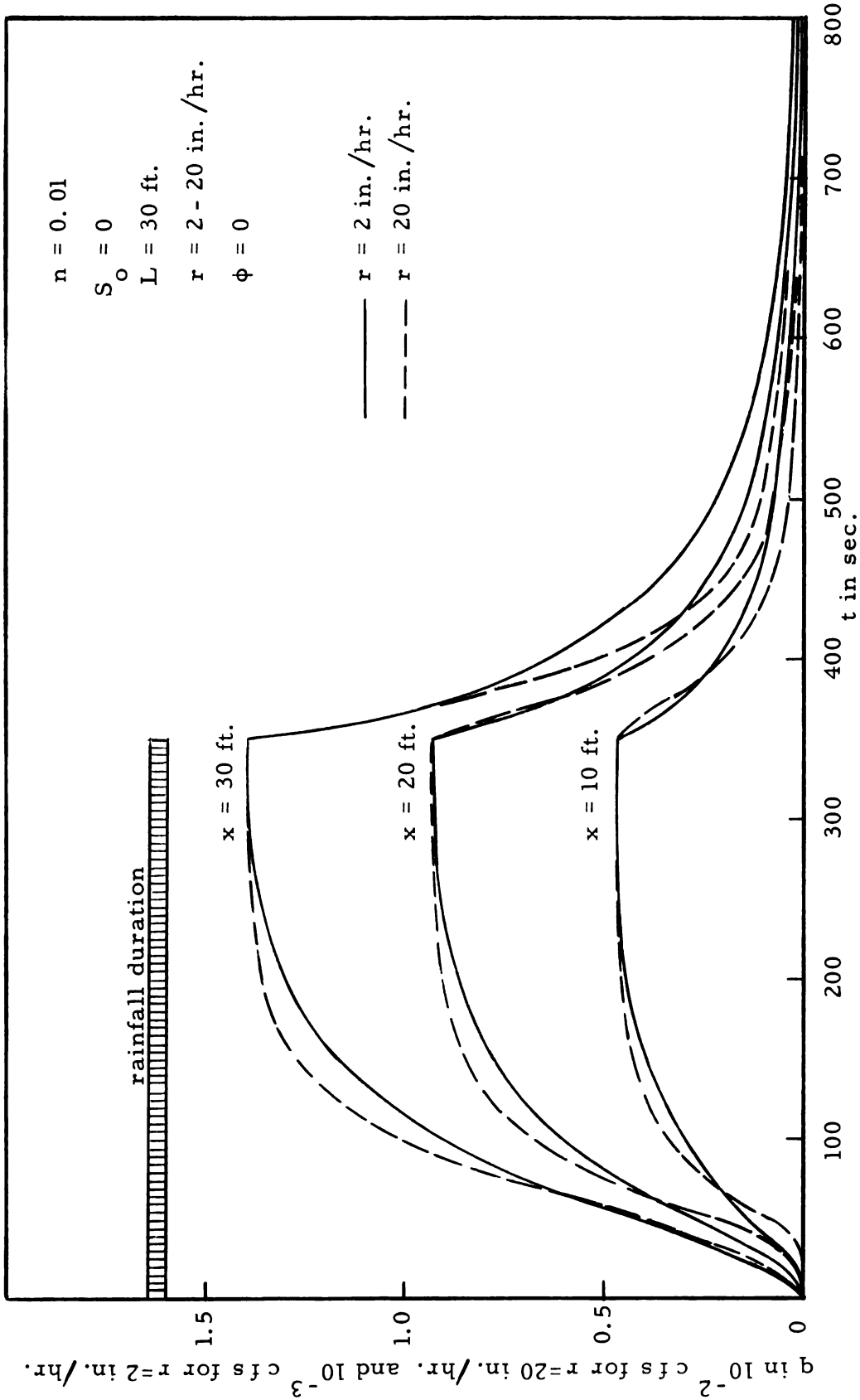


Fig. 20. Comparison of discharge - hydrographs due to different intensities of rainfall.

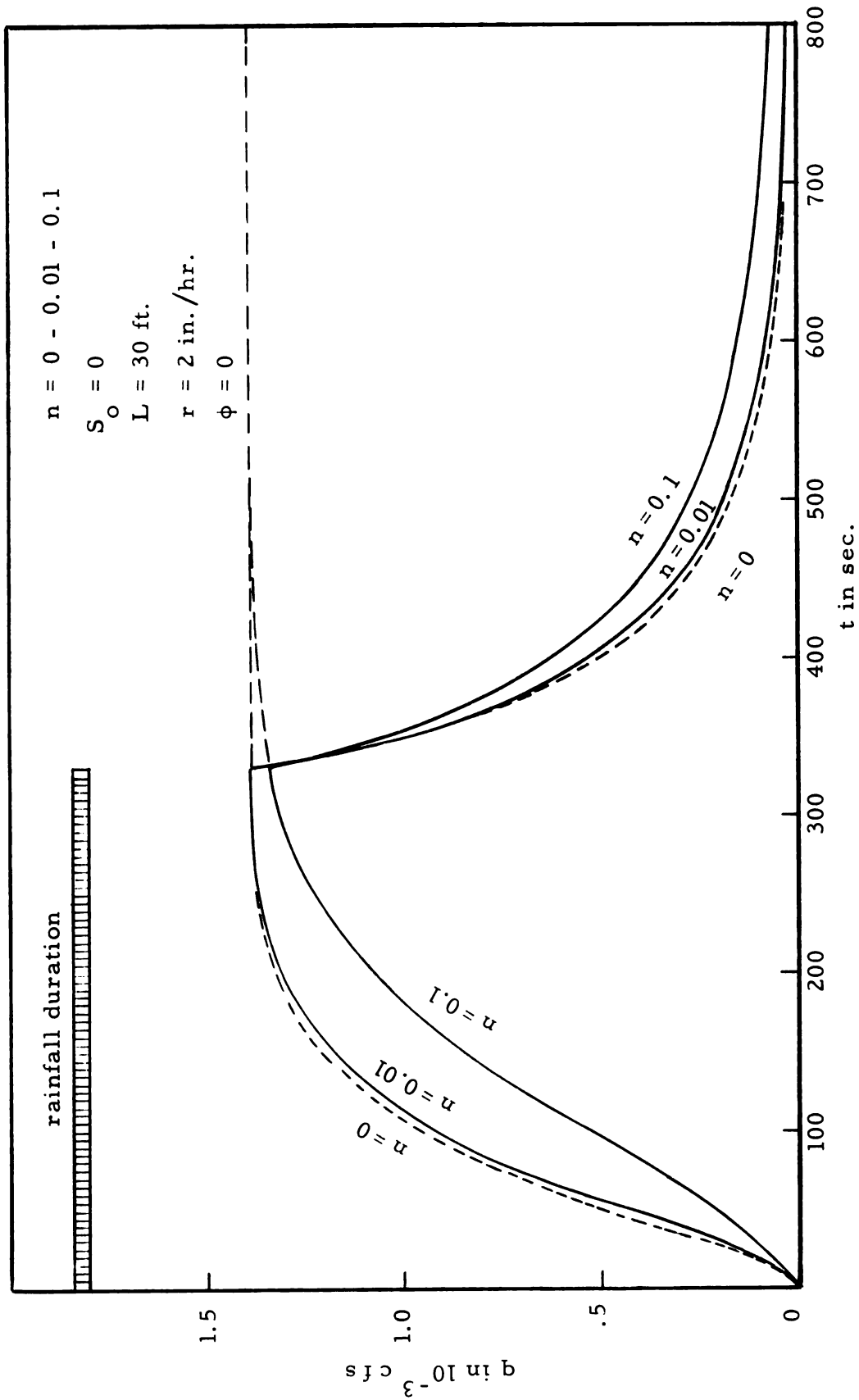


Fig. 21. Comparison of discharge - hydrographs due to different roughnesses at the overfall.

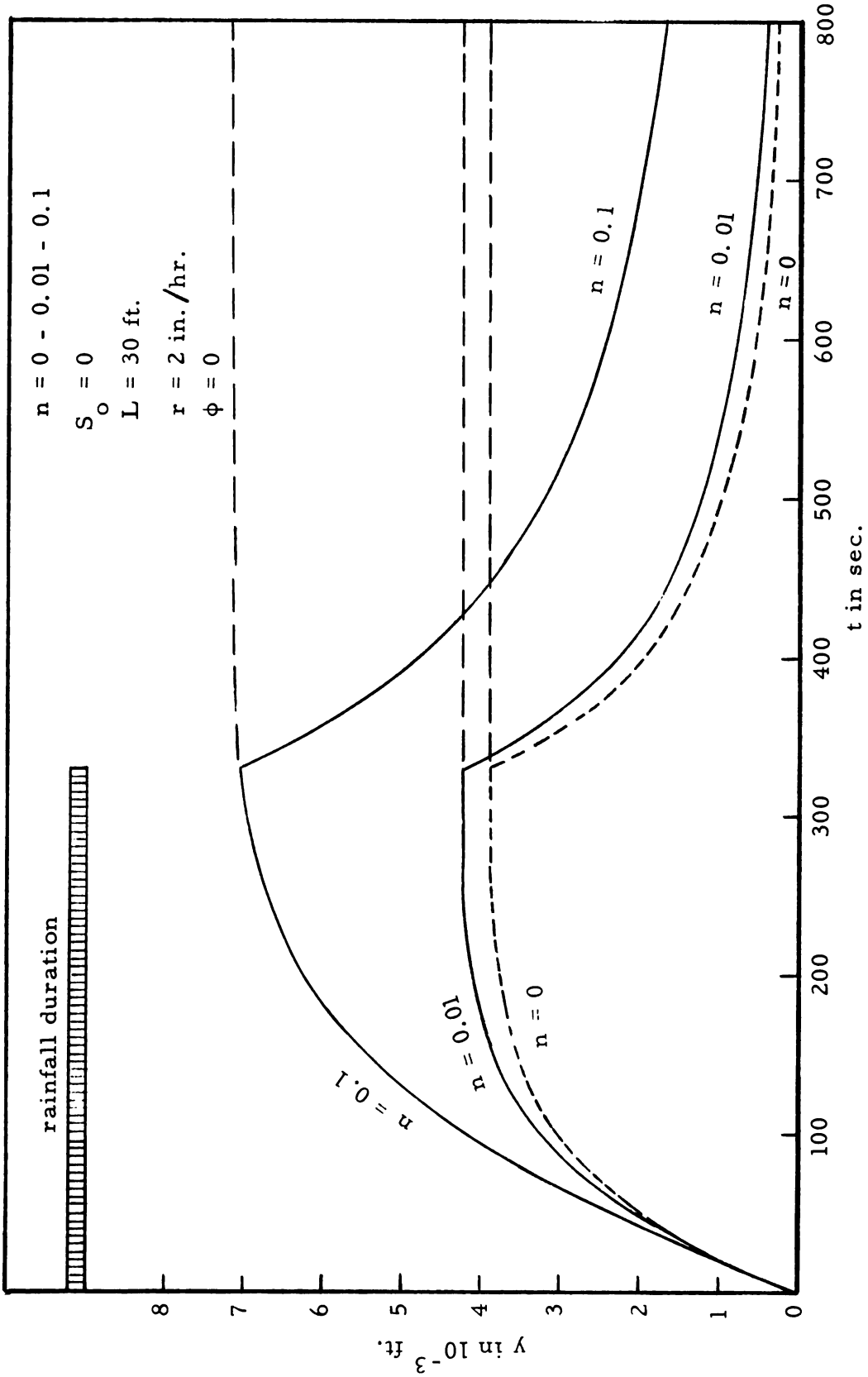


Fig. 22. Comparison of depth - hydrographs due to different roughnesses at the upstream end.

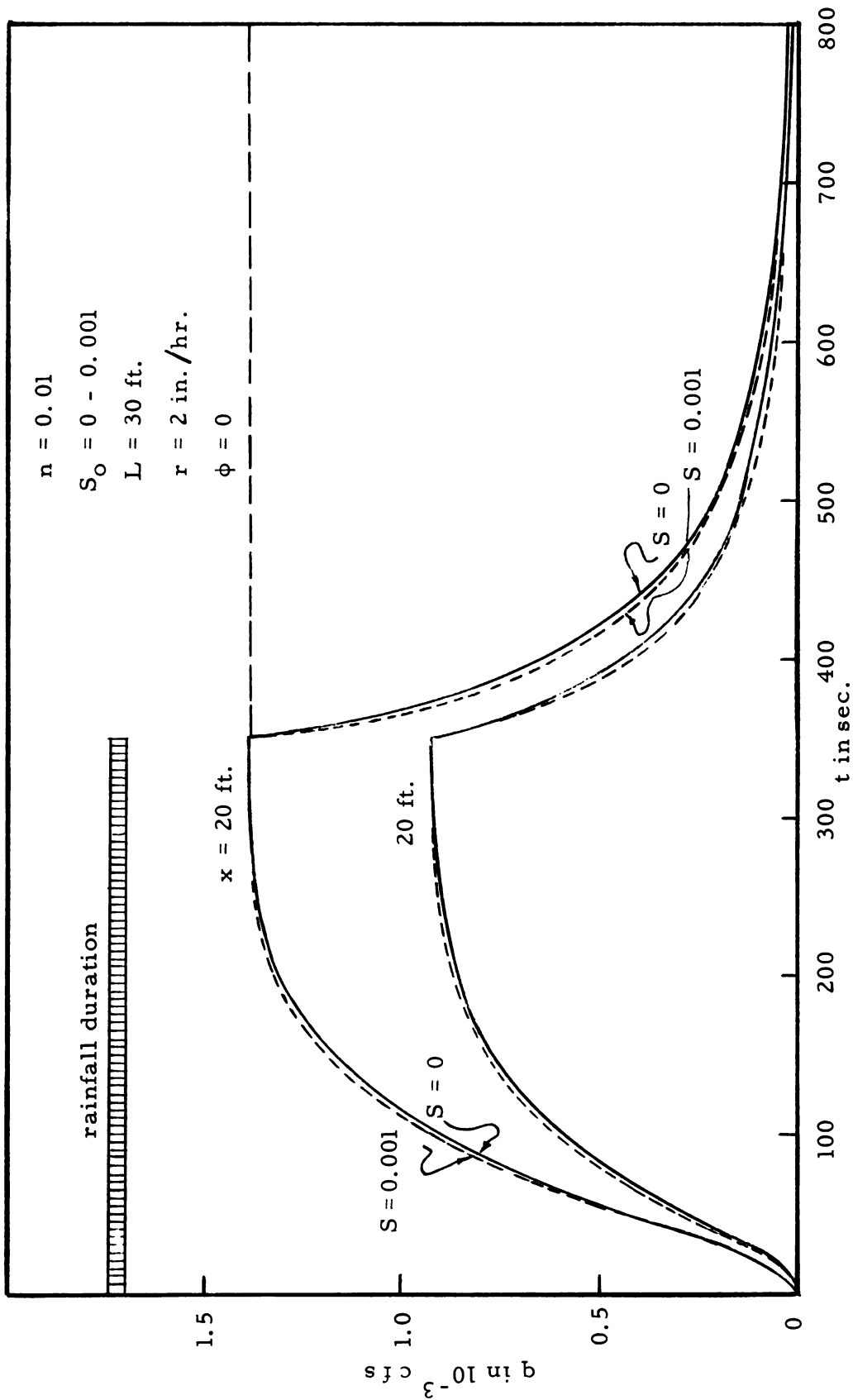


Fig. 23. Comparison of discharge - hydrographs due to different slopes.

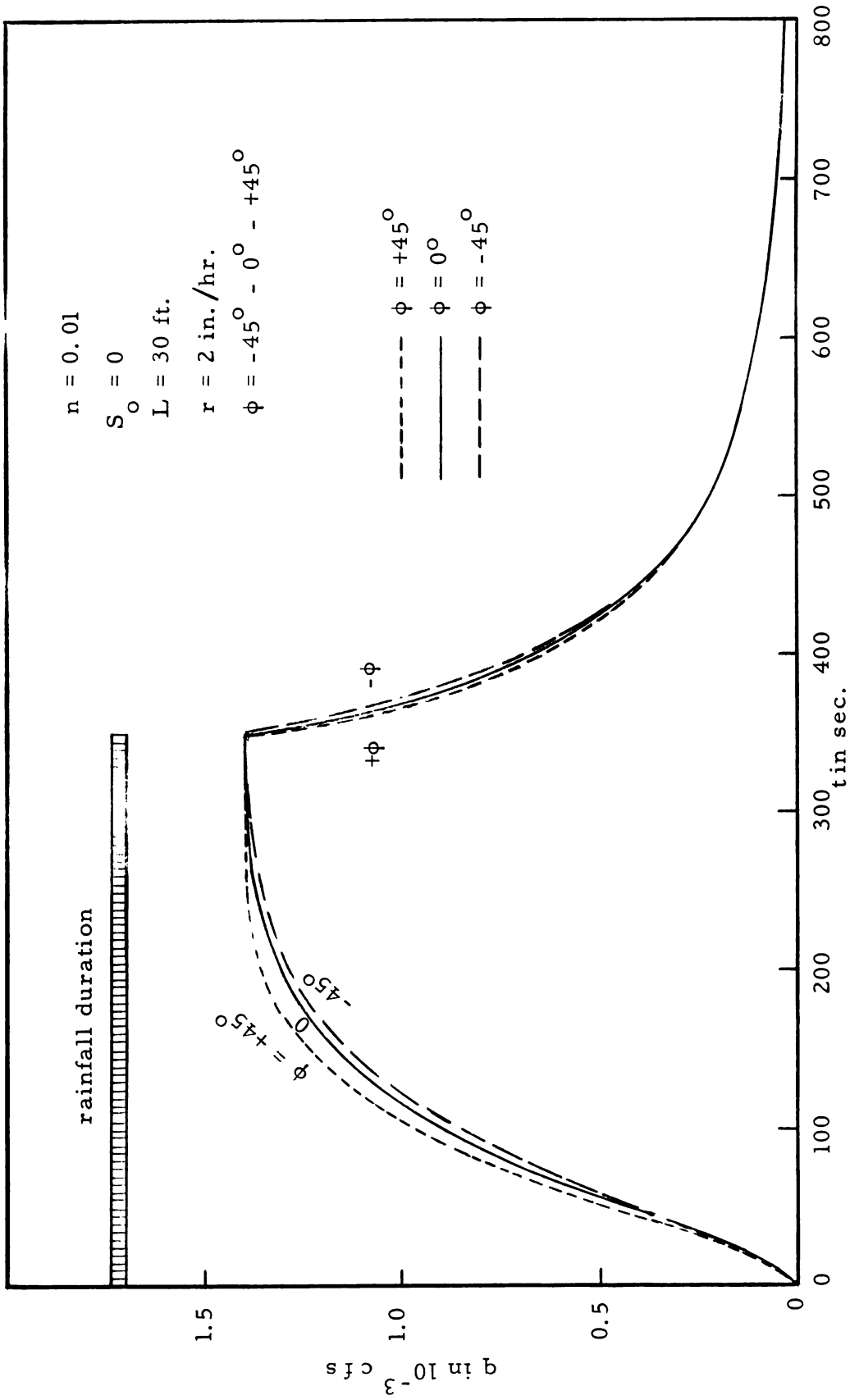


Fig. 24. Comparison of discharge - hydrographs due to different inclinations of rainfall.

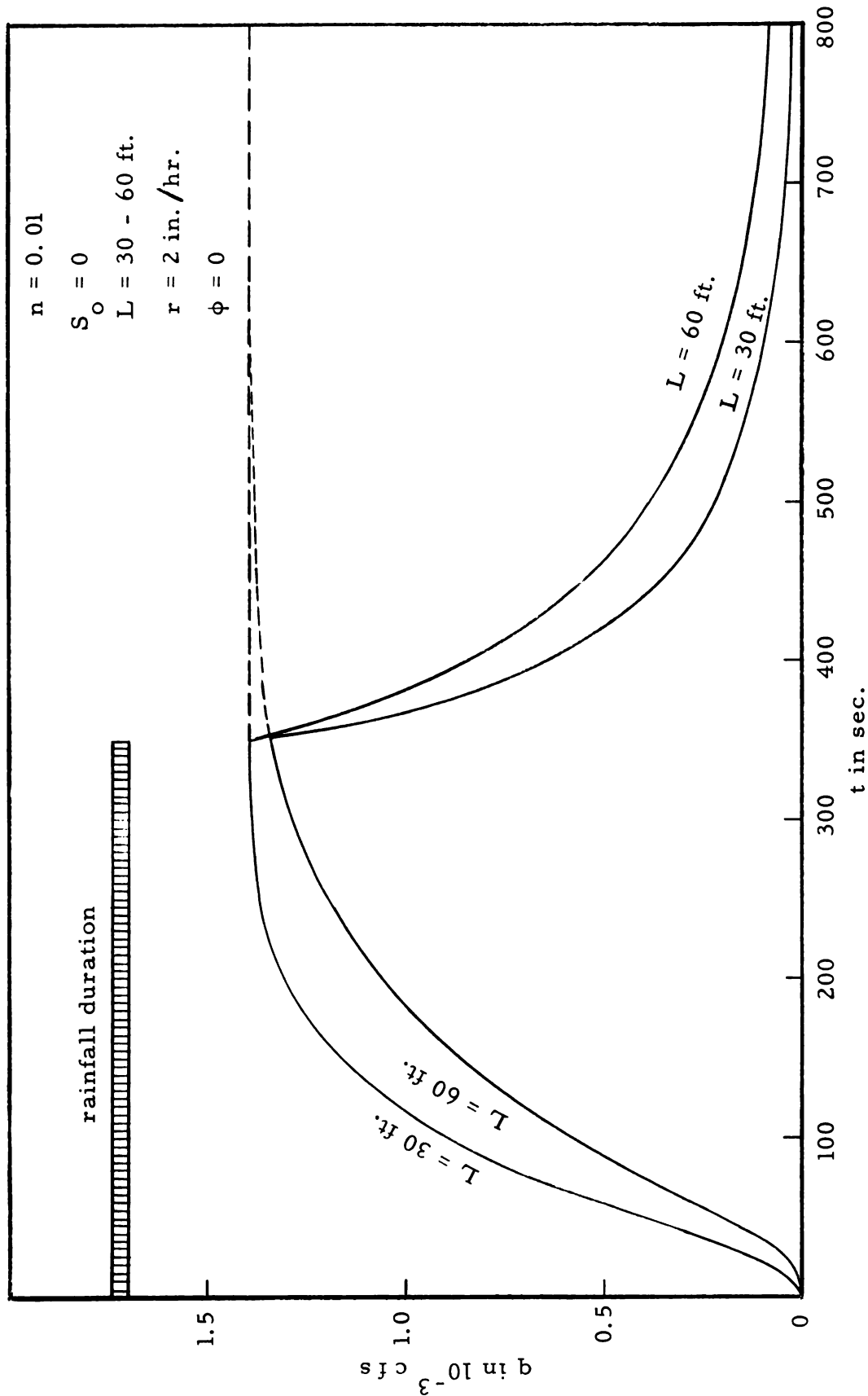


Fig. 25. Comparison of discharge - hydrographs at $x = 30 \text{ ft.}$ due to different lengths of channel.

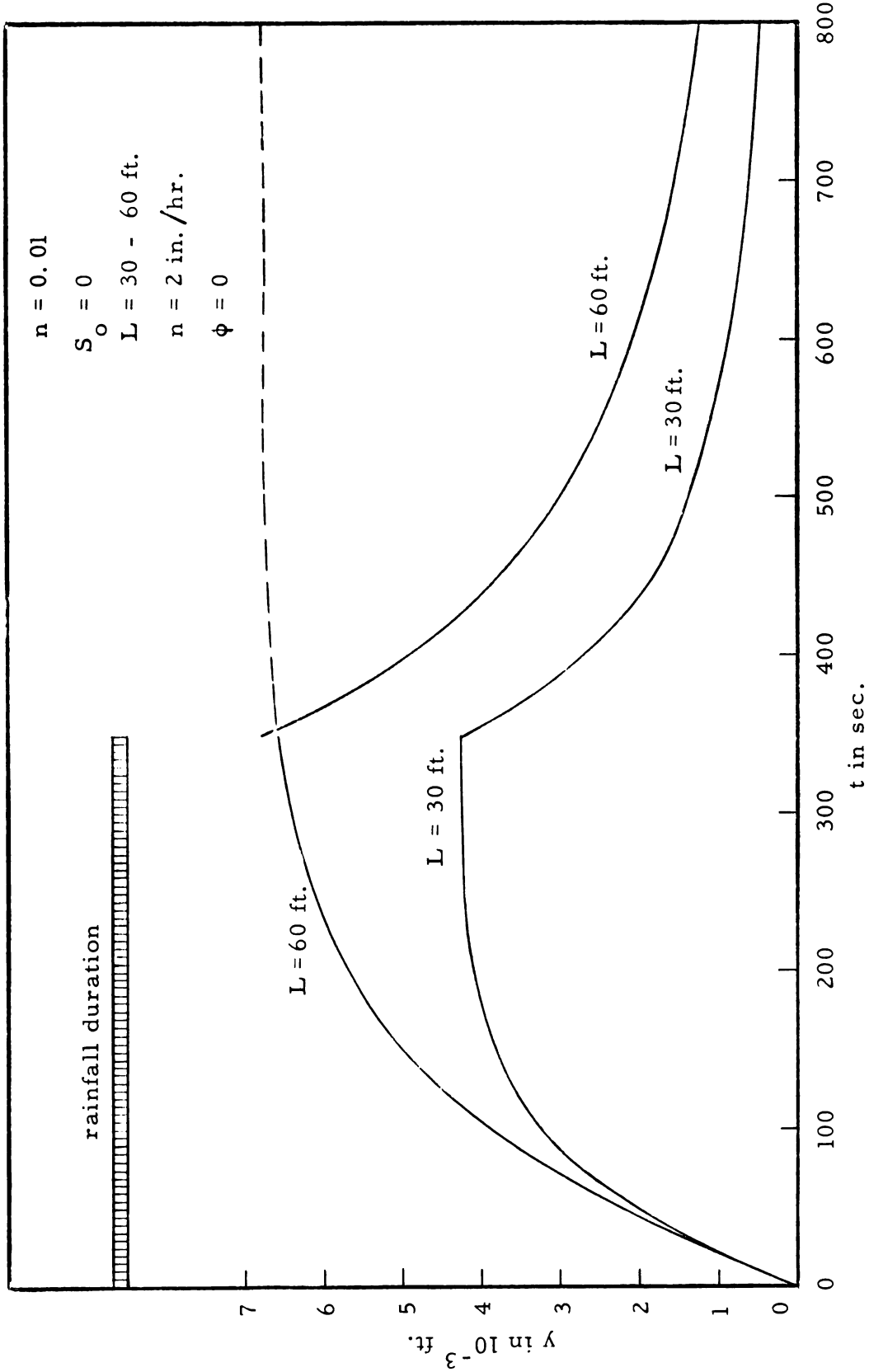


Fig. 26. Comparison of depth - hydrographs at $x = 30 \text{ ft.}$ due to different lengths of channel.

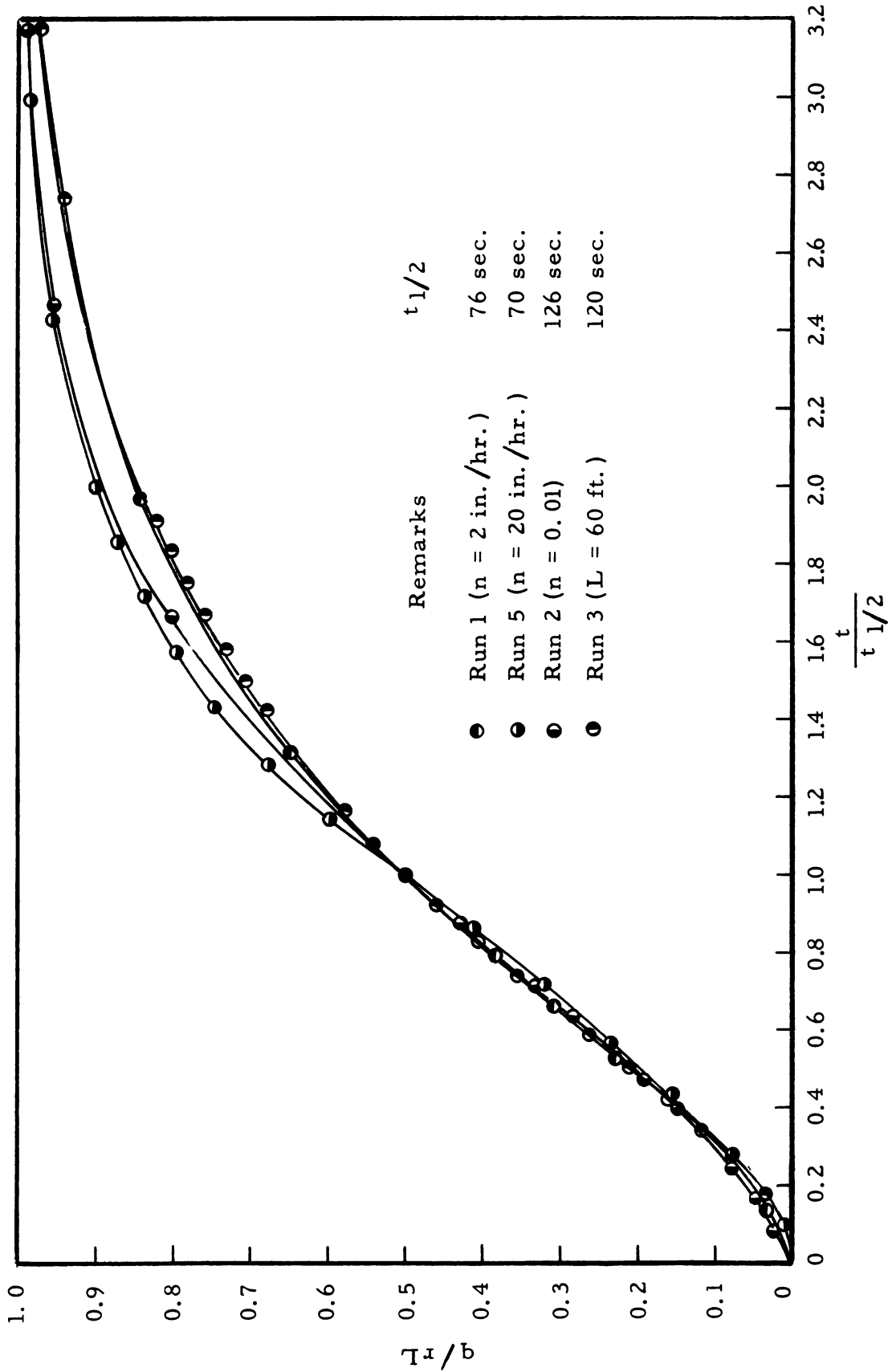


Fig. 27. Dimensionless discharge at the overfall q/rL against the dimensionless time $t/t_{1/2}$.

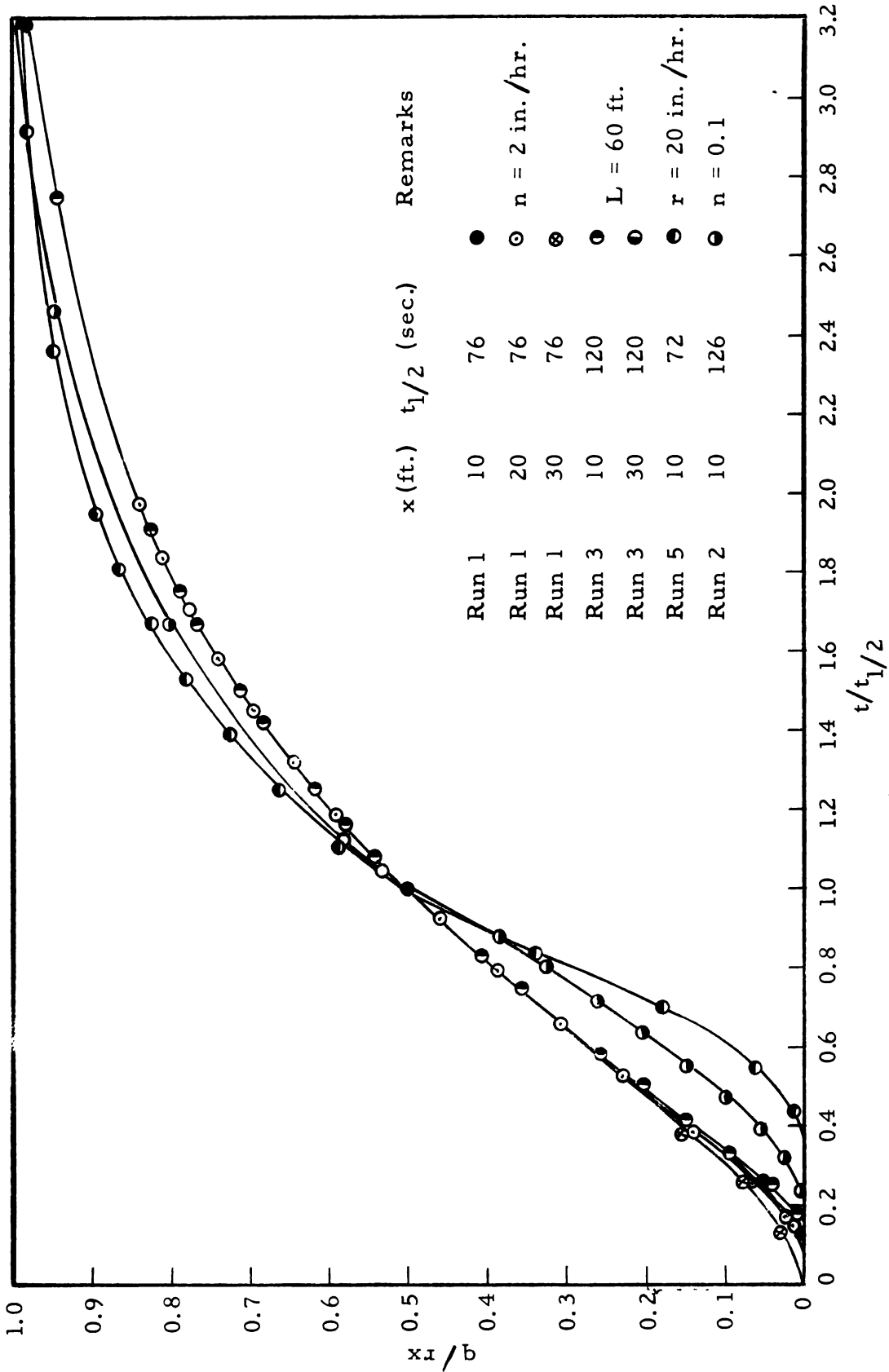


Fig. 28. Dimensionless discharge q/rx against the dimensionless time $t/t_{1/2}$.

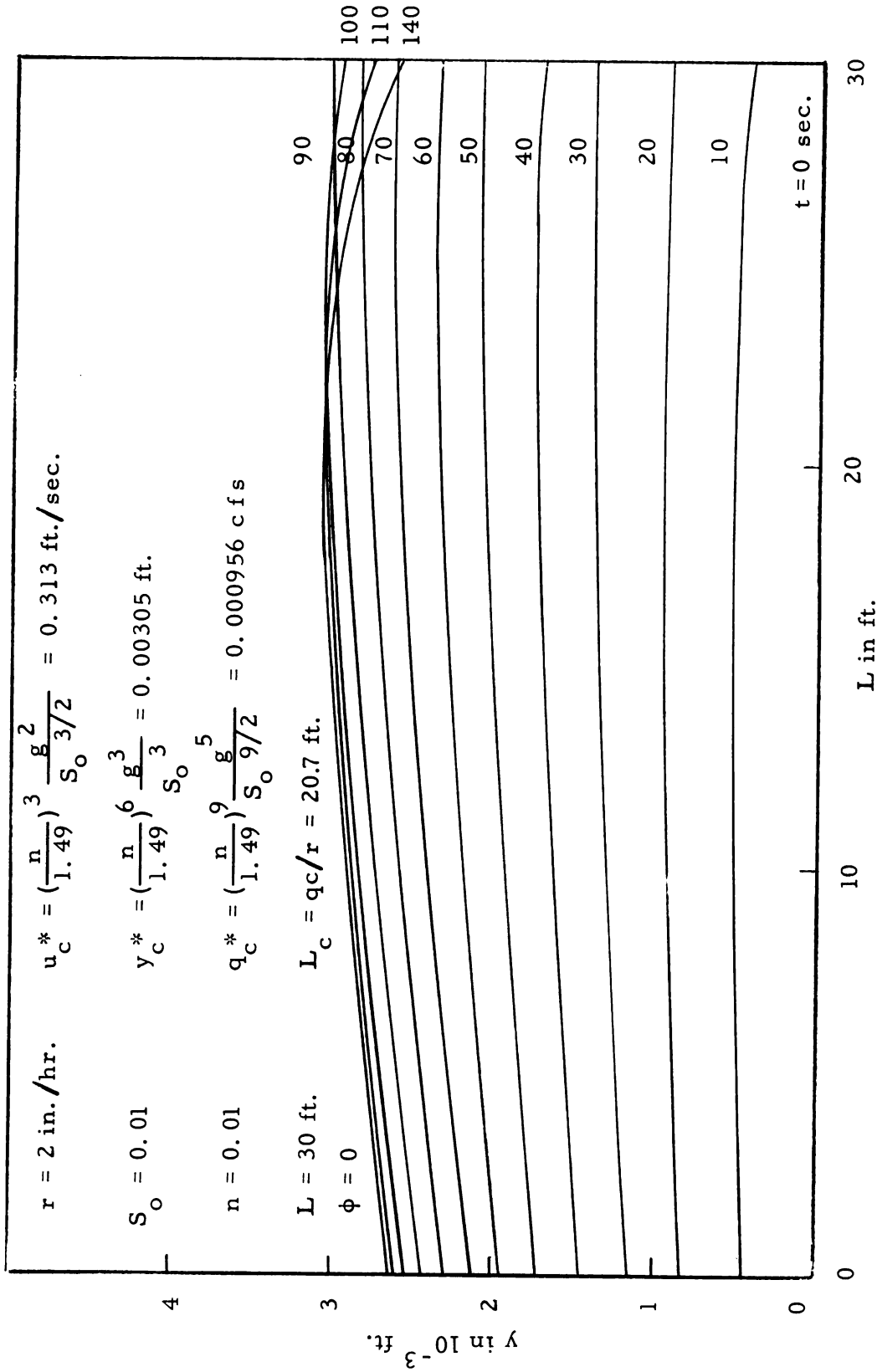


Fig. 29. Depth - profiles of a mixed flow.

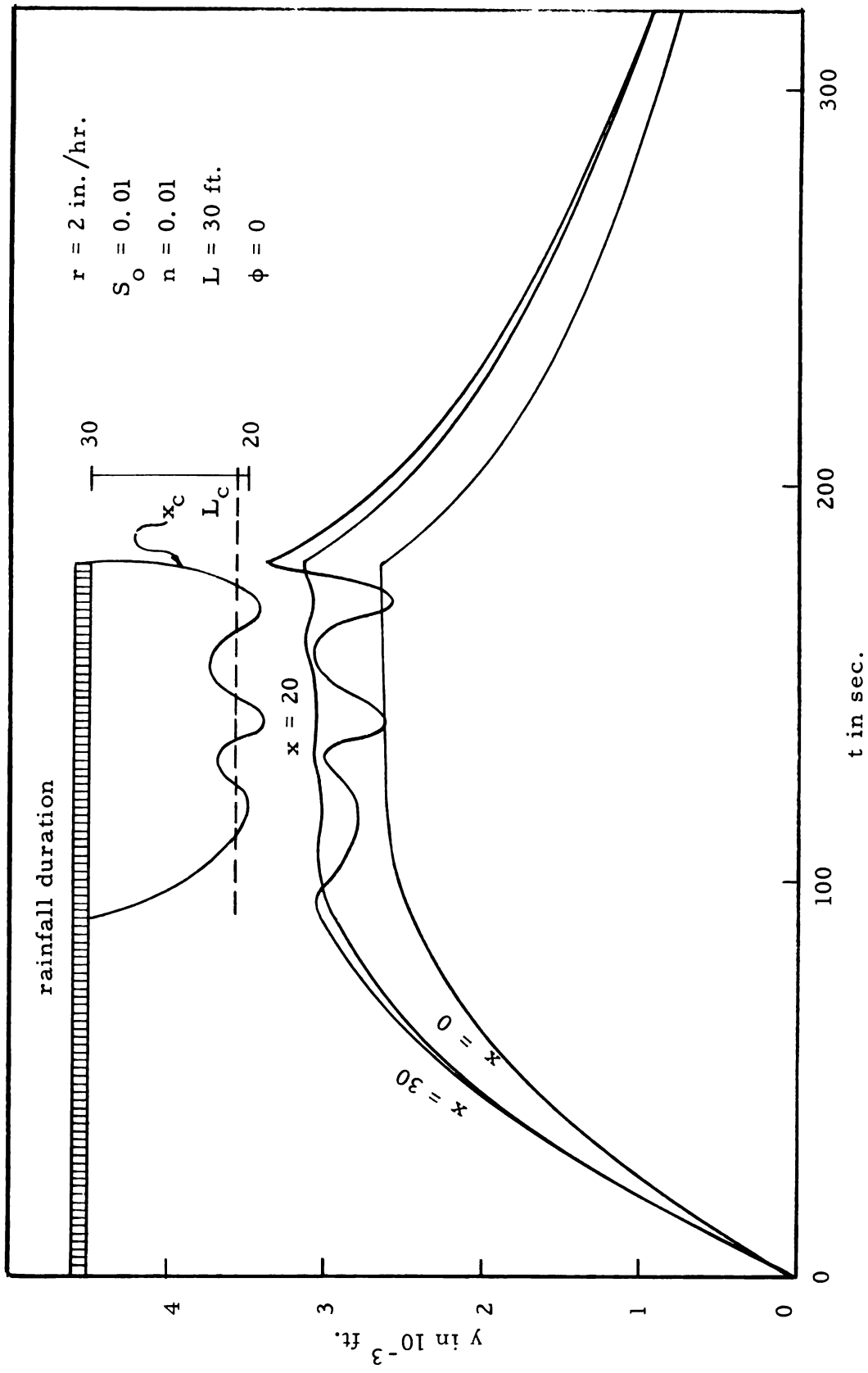


Fig. 30. Stage - hydrographs of a mixed flow.

APPENDIX

Nomenclature

c	Celerity of a shallow water gravity wave = \sqrt{gy}
g	Gravity acceleration
L	Channel length
L_c	Critical channel length = q_c^*/r
M	Momentum flux of the fluid element in the x-direction
n	Manning's number
P	Pressure force on a normal section of the fluid element
q	Discharge per unit width
q_c	Critical discharge per unit width = $\left(\frac{n}{1.49}\right)^9 \frac{g^{5/2}}{S_c}$
q_c^*	Maximum critical discharge per unit width = $\left(\frac{n}{1.49}\right)^9 \frac{g^{5/2}}{S_o}$
$q_{i,j}$	Discharge per unit width at $x = i\Delta x$ and $t = j\Delta t$
$q_{c,j}$	Critical discharge per unit width at $x = x_c$ and $t = j\Delta t$
r	Intensity of rainfall
S_c	Critical slope
S_f	Friction slope as defined by Manning's formula = $\left(\frac{n}{1.49}\right)^2 \frac{u^2}{y^{4/3}}$
S_o	Slope of the channel surface
t_j	time = $j\Delta t$

Δt	Infinitesimal time increment
$t_{1/2}$	Time to reach one-half of the steady state discharge used as the unit of time
$t_{1/4}$	Time to reach one-quarter of the steady state discharge
$t_{3/4}$	Time to reach three-quarters of the steady state discharge
u	Mean velocity in the direction of x axis
u_c	Critical flow velocity in x -direction = $\left(\frac{n}{1.49}\right)^3 \frac{g^2}{S_c^{3/2}}$
u_c^*	Maximum critical flow velocity in x -direction = $\left(\frac{n}{1.49}\right)^3 \frac{g^2}{S_o^{3/2}}$
$u_{i,j}$	Velocity at $x = i\Delta x$ and $t = j\Delta t$
$u_{c,j}$	Critical velocity at $x = x_c$ and $t = j\Delta t$
v	Fall velocity of raindrops in y -direction
W	Weight of the fluid element per unit length
x	Distance from the origin in the longitudinal direction of the flow
Δx	Infinitesimal length increment
x_i	Distance = $i\Delta x$
x_c	Channel length at the critical section from the origin which equals the critical channel length, L_c when the flow reaches its steady state
y	Flow depth
y_c	Critical depth at the critical section = $\left(\frac{n}{1.49}\right)^6 \frac{g^3}{S_c^3}$

y_c^*	Maximum critical depth = $\left(\frac{n}{1.49}\right)^6 \frac{g^3}{S_o^3}$
y_n	Normal depth of flow on the surface
$y_{i,j}$	Flow depth at $x = i\Delta x$ and $t = j\Delta t$
$y_{c,j}$	Critical depth at $x = x_c$ and $t = j\Delta t$
β	Momentum coefficient
γ	Specific weight of water = ρg
θ	Angle of inclination of the surface
ϕ	Angle of rainfall with respect to the vertical
ρ	Density of fluid
ξ	Coefficient of the supplementary pressure force due to the impact of rainfall
τ	Boundary shear on the fluid element per unit length

ENGR. 114

MICHIGAN STATE UNIVERSITY LIBRARIES



3 1293 02723 9338